INVESTIGATION OF THE OBSERVABILITY OF A SATELLITE CLUSTER IN A NEAR CIRCULAR ORBIT

THESIS

Sherrie Norton Filer
Captain, USAF

AFIT/GA/ENY/89D-2

DEPARTMENT OF THE AIR FORCE
AIR UNIVERSITY
AIR FORCE INSTITUTE OF TECHNOLOGY

Wright-Patterson Air Force Base, Ohio

AFIT/GA/ENY/89D-2

INVESTIGATION OF THE OBSERVABILITY OF A SATELLITE CLUSTER IN A NEAR CIRCULAR ORBIT

THESIS

Presented to the Faculty of the School of Engineering
of the Air Force Institute of Technology
Air University
In Partial Fulfillment of the
Requirements for the Degree of
Master of Science in Astronautical Engineering

Sherrie Norton Filer, B.S.
Captain, USAF

December, 1989

Preface

The purpose of the study was to investigate the ability of a Kalman filter to determine the relative position of satellites operating in a cluster environment. The investigation is a follow-on to a study presented by Captain Michael Ward in December 1988 and includes the addition of other forms of measurement data to the filter and a study of the observability of the state components.

I would like to thank everyone that made thesis effort possible. My husband who has provided me with the needed support and encouragement and at times the necessary holds to allow me to complete this work. His ability to find computer resources and his contacts in the computer center became invaluable when our computer and printer were hit by lightning and destroyed. I would also like to thank the people in the graphic laboratory who sort of adopted me and allowed me to use their abundant resources. Special thanks goes to my advisor, Dr. William Wiesel whose knowledge and understanding were greatly appreciated when the testing of the filter did not go according to plan and frustration was beginning to set in. The final person I must thank is my chiropractor, Dr. Richard Teeters who was there at least twice a week for me, and whose amazing hands allowed me to continue working.

Sherrie Norton Filer

Table of Contents

List of Figures

Abstract

The relative position determination of a cluster of satellites in a near circular orbit was investigated in a thesis by Captain Michael L. P. Ward in December 1988. His investigation involved the use of dynamics based on the Clohessy-Wiltshire equations and an on-board estimator based on the U-D covariance factorization version of the Kalman filter. The initial performance results proved favorable, with the filter meeting the required 25 meter accuracy in all test cases. The purpose of this thesis is to validate the test results achieved by Captain Ward and to investigate the ability of the filter to determine the relative position of the satellites to a higher degree when the filter in use is not resident on that satellite. This investigation included the use of additional measurement data from other satellites in the cluster to the Kalman filter for processing in the update cycle. When it was determined that the measurements were not allowing satellite 1 to update, the observability of the components of the state vector were computed and the results discussed.

INVESTIGATION OF THE OBSERVABILITY OF A SATELLITE CLUSTER IN A NEAR CIRCULAR ORBIT

I. Introduction

The construction of a group of satellites into clusters has been under investigation in the area of satellite communications for several years (5:831). A cluster is defined as an array of two or more satellites located in a specified orbital area, that appear and operate as one to an Earth-based user. The amount of separation allowed between satellites is determined by its application and the accuracy of the orbital control method. The benefits to employing this strategy are numerous. By dividing the work load between satellites, the entire system can provide a service greater than each individual satellite. The entire system is more reliable due to the availability of in-orbit spares and survivability is enhanced because destroying one satellite does not destroy the entire system.

There are several problems that need to be addressed in order for this cluster strategy to work. These areas include cooperative orbit control strategies, cluster geometry and orbit determination. This thesis is concerned only with the problem of accurately determining the relative position of each satellite. The stochastic nature of this position determination problem has previously been address by author John Murdoch in several articles (7:1001-1018). His method of analysis used a least squares algorithm, which is less appropriate than a recursive filter for on-board applications, and his cluster size was limited to two satellites. This thesis determines the position of up to ten satellites in a cluster and uses a recursive Kalman filter to estimate the position of the satellites (5:1006). The approach presented in this study takes the

pulses used by each satellite to synchronize their on-board clocks to provide input to a Kalman filter for satellite relative position determination. This filter was designed for satellite 1 but can easily be adjusted for use with any of the members of the cluster by having each satellite think it is number 1. The assignment of numbers to the satellites is an arbitrary designation since the cluster geometry is randomly determined by Equation (3).

The proposed use of this Kalman filter is in a cluster designed as a space based radar. In order for the radar to form a cohesive image, the relative position of each satellite needs to be known to at least one quarter of a wavelength. At the one quarter limit however, the resultant fogginess and loss of contrast are appreciable and can affect the visibility of very fine detail (2:443-444). Since the military requirements of a phased array radar may include the need for fine detail, the tolerance will be decreased to one tenth of a wavelength or 21.6 meters. The method used to obtain this value is presented in Appendix A.

The study presented by Captain Michael Ward proved that the concept of using a recursive filter to determine relative position is, under initial testing, viable (8:1-1-4-1). The purpose of this thesis is to continue the testing of the U-D covariance factorization Kalman filter (3:392-400), to include determining filter error statistics and to perform an investigation of the discrepancy between the results achieved for satellite 1 and those achieved for other members of the cluster. The measure of performance will be the comparison of the average of the standard deviations extracted from the eigenvalues of the position covariance matrix to the statistics of the true error. The true error is defined as the root-mean-square of the relative position components computed from the estimated state provided by the filter and the actual state provided by the truth model. For this performance investigation the cluster was placed in near-circular, low-earth orbit. (8:1-2).

II. Background

Since this thesis is a continuation of Captain Michael Ward's work, the development of the initial Kalman filter and truth model will be represented in less detail. For a more detailed analysis of the filter development, the reader should consult the Ward thesis (8). The truth model was based on an array of from one to ten satellites orbiting the earth with the same orbital period. The truth model was limited to the two body equations of motion and had as output the true state $x_t(t)$, whose components are the relative position and velocity of each satellite with respect to a rotating reference point, and the satellites relative position measurement $z_t(t)$. This relative measurement data was then used by the Kalman filter to determine an estimated state $\hat{x}(t)$. The position elements of the true state were then compared to those of the estimated state for each satellite to provide the true error of the system $e_t(t)$. A diagram of the filter is presented in Figure 1.

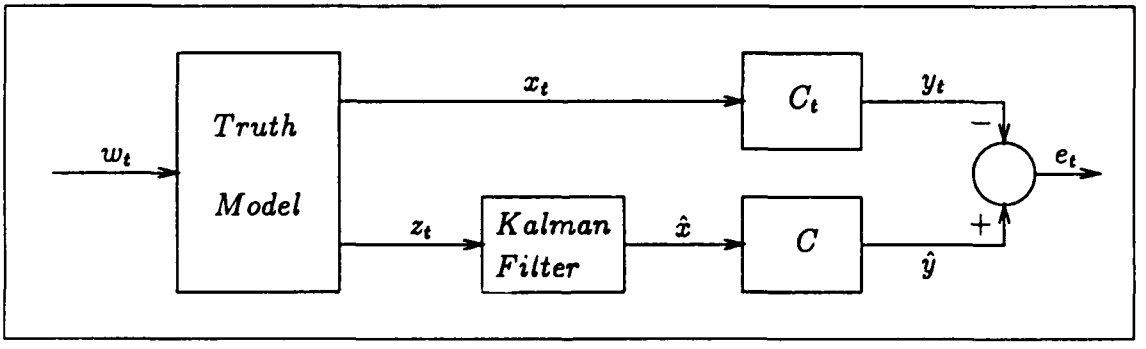

Figure 1. Kalman Filter

The true error statistics were then compared to the average value of the standard deviations defined as the ($\sqrt{eigenvalues}$) of each satellite's position covariance

matrix to determine the filter's performance. The covariance of the filter tells the user how well the filter thinks it is performing.

2.1 Truth Model

The truth model provides the filter with only relative information concerning the position of each of the satellites in the cluster. Since the measurement data is relative, absolute position can not be estimated. Instead the relative position was determined with respect to a rotating reference point. The earth-centered frame $(\hat{i}, \hat{j}, \hat{k})$ is considered inertial and the reference frame $(\hat{x}, \hat{y}, \hat{z})$ is rotating with respect to this inertial frame at a constant angular velocity $\omega\,\hat{k}$. The reference point is in a circular orbit with a radius of R and has a circular orbital velocity of $\sqrt{\frac{\mu}{R}}$. This arrangement is shown in Figure 2.

The position and velocity of the reference point in the inertial frame at the initial time (t=0) are:

$$r_{ref} = \begin{bmatrix} R \\ 0 \\ 0 \end{bmatrix} \tag{1}$$

$$v_{ref} = \begin{bmatrix} 0 \\ v_{cs} \\ 0 \end{bmatrix} \tag{2}$$

The positions of the satellites were determined at random about the reference point but within a specified radius (rad) and the velocity vectors were determined from the Clohessy-Wiltshire equations (10:80). These equations have the following form:

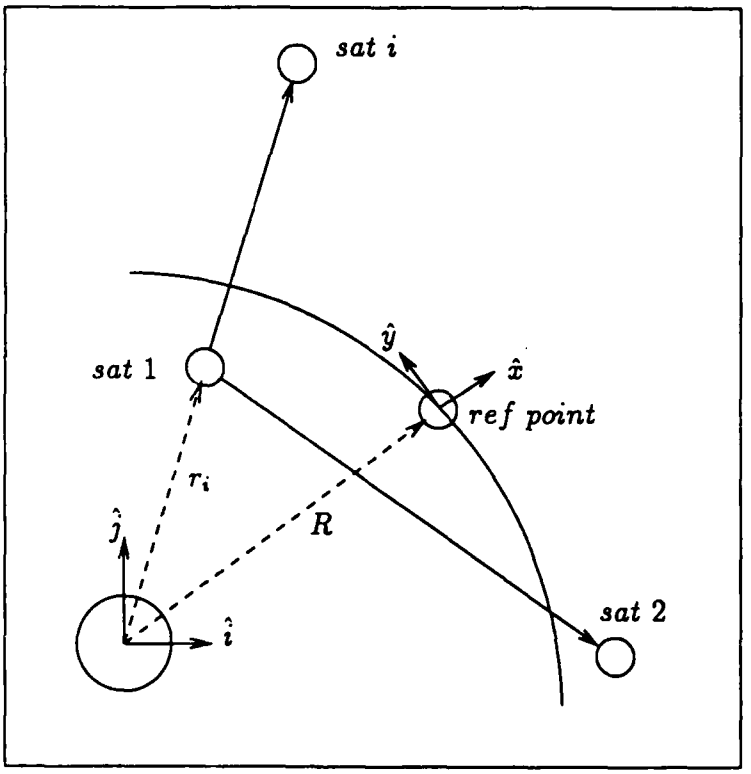

Figure 2. Reference System

$$r_i = \begin{bmatrix} R \\ 0 \\ 0 \end{bmatrix} + n_i * (rad) \tag{3}$$

$$v_i \hat{i} = \eta \left(r_i \hat{i} - r_{ref} \hat{i} \right) \tag{4}$$

$$v_i \hat{j} = (2\,\mu(\frac{1}{r_1} - \frac{1}{2a}) - v_i^2 \hat{i} - v_i^2 \hat{k})^{\frac{1}{2}} \tag{5}$$

$$v_i \hat{k} = \eta r_i \hat{k} \tag{6}$$

where n_i is the output of a uniformly distributed random number generator with outputs between -0.5 and 0.5 and η is defined as the mean motion.

The input for the Kalman filter can be formed using this position and velocity information. The true initial state $x_t(t = 0)$ is defined as the position and velocity of each satellite in the rotating frame. Since the coordinate frames are initially aligned, the position of each satellite in the rotating frame is:

$$r_{i[rot]} = (r_i - r_{ref})_{fix} \tag{7}$$

The velocity expressed in term of relative position is:

$$v_{i[rot]} = (v_i - v_{ref})_{[fix]} - \omega \times r_{i[rot]} \tag{8}$$

Ward discovered in his thesis that the absolute downrange position y was unobservable. The downrange component was removed from satellite 1 and the state of satellites 2 through s were modified to include the relative (Δy_i) rather than the absolute downrange component, where Δy_i is defined as:

$$\Delta y_i = y_1 - y_i \tag{9}$$

with $i = 2, 3, ..., s$. Figures 3 and 4 show the x and y components of the state with and without this modification. The z component is normal to the plane of the page and was not affected by the modification.

With this modification the state vectors in the rotating reference frame are defined as:

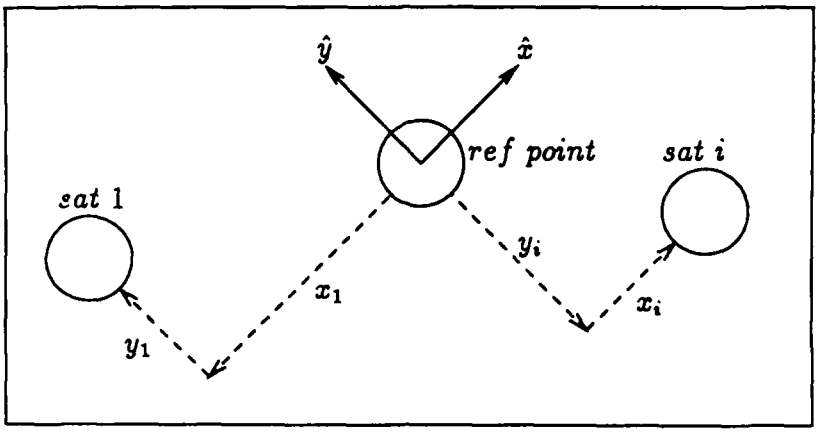

Figure 3. The Original Component Representation of the Cluster

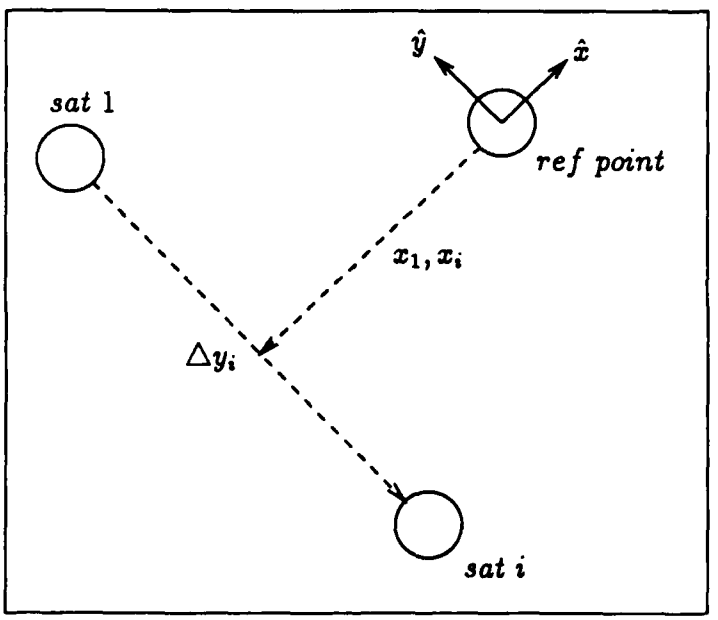

Figure 4. The Modified Component Representation of the Cluster

$$x_1 = \begin{bmatrix} x_1 \\ z_1 \\ \dot{x}_1 \\ \dot{y}_1 \\ \dot{z}_1 \end{bmatrix} \quad and \quad x_i = \begin{bmatrix} x_i \\ \triangle y_i \\ z_i \\ \dot{x}_i \\ \dot{y}_i \\ \dot{z}_i \end{bmatrix} \tag{10}$$

The relative measurement vector has the following form:

$$z_t = \begin{bmatrix} | r_1 - r_2 | \\ \vdots \\ | r_1 - r_s | \end{bmatrix} + u_t \tag{11}$$

where u_t is a zero-mean, white Gaussian noise diagonal matrix with a covariance of R_t (3:330). The values for the covariance R_t were determined by the Ward thesis to be .01 meters. This value was probably obtained from the satellite with largest true error calculated once the filter was tuned. Statistically, this allows the advertised error in the measurements to match the actuals error in the position of the satellites. The noise u_t, represents the errors in computing the range measurements from one satellite to the others. The major errors result from clock synchronization differences between satellites as well as resolution limitations of the on-board clock (7:1016). These errors were also considered to be independent from measurement to measurement and were therefore grouped together as one error term along the diagonals of the measurement covariance matrix.

The solution to the Kepler problem is used to determine the future position and velocity of each satellite. The Kepler problem is solved using the f and g equations in terms of the *eccentric anomaly* E (1:219). These equations have the following form:

$$f = 1 - \frac{a}{r_0}(1 - \cos \triangle E) \tag{12}$$

$$g = t - \sqrt{\frac{a^3}{\mu}}(\triangle E - \sin \triangle E) \tag{13}$$

$$\dot{f} = -\frac{\sqrt{\mu a} \sin \triangle E}{r r_0} \tag{14}$$

$$\dot{g} = 1 - \frac{a}{r}(1 - \cos \triangle E) \tag{15}$$

where $\triangle E$ and r are defined as:

$$\triangle E = E_f - E_0 \tag{16}$$

$$r = a(1 - \epsilon \cos E_f) \tag{17}$$

The value for E_f was determined through the use of a Newton iteration method since the *eccentric anomaly* does not have a closed form solution (9:61). A more detailed description of this process is presented in the Ward thesis (8:2-6-2-7). Once the f,g,$\dot{f}$ and $\dot{g}$ variables have been computed the new position and velocity can be determined using the following equations:

$$r(t) = f r_0 + g v_0 \tag{18}$$

$$v(t) = \dot{f} r_0 + \dot{g} v_0 \tag{19}$$

Once the position and velocity of each satellite in the inertial frame have been determined, the relative position to the reference point can be found. The first step is to determine the inertial position and velocity of the reference point. Defining θ as ωt, the position and velocity vectors are:

$$r_{ref[fix]}(t) = \begin{bmatrix} R\cos\theta \\ R\sin\theta \\ 0 \end{bmatrix} \tag{20}$$

$$v_{ref[fix]}(t) = \begin{bmatrix} -v_{cs}\sin\theta \\ v_{cs}\cos\theta \\ 0 \end{bmatrix} \tag{21}$$

The next step is to determine the relative distance between the reference point and each satellite in the inertial frame. Using the position and velocity of the satellites, computed from the *eccentric anomaly*, and the position and velocity of the reference point listed above, the relative distance becomes

$$r_{rel[fix]} = [r(t) - r_{ref}(t)] = r_1\,\hat{i} + r_2\,\hat{j} + r_3\,\hat{k} \tag{22}$$

$$v_{rel[fix]} = [v(t) - v_{ref}(t)] = v_1\,\hat{i} + v_2\,\hat{j} + v_3\,\hat{k} \tag{23}$$

Since the inertial and rotating reference frames are no longer aligned, a coordinates transformation must be performed to obtain the relative distance in the noninertial frame. Performing this transformation yields:

$$\begin{bmatrix} r_{rel[rot]} \\ v_{rel[rot]} \end{bmatrix} = \begin{bmatrix} r_1\cos\theta + r_2\sin\theta \\ -r_1\sin\theta + r_2\cos\theta \\ r_3 \\ v_1\cos\theta + v_2\sin\theta + \omega r_2 \\ -v_1\sin\theta + v_2\cos\theta - \omega r_1 \\ v_3 \end{bmatrix} \equiv \begin{bmatrix} x \\ y \\ z \\ \dot{x} \\ \dot{y} \\ \dot{z} \end{bmatrix} \tag{24}$$

2.2 *Kalman Filter*

The truth model presented in the last section provides the actual state. The purpose of the Kalman filter is to estimate this state to a predetermined degree of accuracy. This filter performs two functions: the first is to propagate the estimated state and its covariance forward in time, and the second is to update the state and covariance using the measurement data provided by the truth model. This cluster system is represented in the form of a linear stochastic differential equation which describes the state propagation, with discrete-time, noise corrupted, nonlinear inputs as available data (8:2-10).

2.2.1 State Propagation and Update .

Since the dynamics used to propagate the state are discrete-time and linear, the underlying dynamics model has the following form:

$$x(t_i) = \Phi(t_i, t_{i-1})x(t_{i-1}) + G_d(t_{i-1})w_d(t_{i-1}) \tag{25}$$

where w_d is a discrete-time, zero-mean, white Gaussian noise sequence with covariance equal to the dynamics driving noise Q_d at time equals t_i, and G_d is assumed to be the identity matrix for an equivalent discrete-time model (3:220). The Φ matrix represents the state transition matrix of the system and will be defined in more detail later in this section. This equation leads to the standard filter propagation equation for the Kalman filter defined as (3:220):

$$\hat{x}(t_i^-) = \Phi(t_i, t_{i-1})\,\hat{x}(t_{i-1}^+) \tag{26}$$

where (t^-) and (t^+) represent the state before and after the update. For convenience, they will be represented as $(-)$ and $(+)$ for the remainder of this thesis. Each satellites Φ matrix is determined from the Clohessy-Wiltshire equations of motion, with η representing the mean motion (10:80). These equations are:

$$\ddot{x} - 2\eta\dot{y} - 3\eta^2 x = 0 \tag{27}$$

$$\ddot{y} + 2\eta\dot{x} = 0 \tag{28}$$

$$\ddot{z} + \eta^2 z = 0 \tag{29}$$

The above equations are valid for small displacements in the radial and out-of-plane directions but remain correct for large changes in the in-track direction (10:80). These equations of motion are integrated about the initial conditions x_0,$\dot{x}_0$,y_0,$\dot{y}_0$, etc. at $t = 0$ to obtain the following position and velocity solutions (8:2-12):

$$x(t) = -\left(\frac{2}{\eta}\dot{y}_0 + 3x_0\right)\cos\eta t + \frac{\dot{x}_0}{\eta}\sin\eta t + 4x_0 + \frac{2}{\eta}\dot{y}_0 \tag{30}$$

$$y(t) = y_0 - (3y_0 + 6\eta x_0)t + \left(\frac{4\dot{y}_0}{\eta} + 6x_0\right)\sin\eta t + \frac{2\dot{x}_0}{\eta}\cos\eta t - \frac{2\dot{x}_0}{\eta} \tag{31}$$

$$z(t) = z_0\cos\eta t + \frac{\dot{z}_0}{\eta}\sin\eta t \tag{32}$$

$$\dot{x}(t) = (2\dot{y}_0 + 3\eta x_0)\sin\eta t + \dot{x}_0\cos\eta t \tag{33}$$

$$\dot{y}(t) = -3\dot{y}_0 - 6\eta x_0 + (6\eta x_0 + 4\dot{y}_0)\cos\eta t - 2\dot{x}_0\sin\eta t \tag{34}$$

$$\dot{z}(t) = -z_0\eta\sin\eta t + \dot{z}_0\cos\eta t \tag{35}$$

Using these equations, the following Φ matrix can be formed for a satellite with six states represented by x,y,z,$\dot{x}$,$\dot{y}$, and $\dot{z}$:

$$\Phi_i = \begin{bmatrix} 4-3\cos\psi & 0 & 0 & \frac{\sin\psi}{\eta} & \frac{2}{\eta}(1-\cos\psi) & 0 \\ 6(\sin\psi-\psi) & 1 & 0 & \frac{2}{\eta}(\cos\psi-1) & \frac{4}{\eta}\sin\psi-\frac{3\psi}{\eta} & 0 \\ 0 & 0 & \cos\psi & 0 & 0 & \frac{\sin\psi}{\eta} \\ 3\eta\sin\psi & 0 & 0 & \cos\psi & 2\sin\psi & 0 \\ 6\eta(\cos\psi-1) & 0 & 0 & -2\sin\psi & -3+4\cos\psi & 0 \\ 0 & 0 & -\eta\sin\psi & 0 & 0 & \cos\psi \end{bmatrix} \quad (36)$$

where $\psi = \eta t$. Since the state vectors were modified to include $\triangle y_i$ instead of y_i, Equation (31) was substituted into Equation (9). For $i = 2, 3, .., s$ this modification yields:

$$\begin{aligned} \triangle y_i(+) &= (6(\sin\psi-\psi))(x_1-x_i) + \triangle y_i + \left[\frac{2}{\eta}(\cos\psi-1)\right](\dot{x}_1-\dot{x}_i) + \\ &\quad \left(\frac{4}{\eta}\sin\psi-\frac{3\psi}{\eta}\right)(\dot{y}_1-\dot{y}_i) \end{aligned} \quad (37)$$

where the components on the right hand side of the equation are evaluated at the previous sample time. Each satellite's Φ matrix can now be formed. Φ_1 is reduced from a 6-by6 to a 5-by-5 by matrix with the row and column corresponding to the y component removed (8:2-19):

$$\Phi_1 = \begin{bmatrix} 4-3\cos\psi & 0 & \frac{\sin\psi}{\eta} & \frac{2}{\eta}(1-\cos\psi) & 0 \\ 0 & \cos\psi & 0 & 0 & \frac{\sin\psi}{\eta} \\ 3\eta\sin\psi & 0 & \cos\psi & 2\sin\psi & 0 \\ 6\eta(\cos\psi-1) & 0 & -2\sin\psi & -3+4\cos\psi & 0 \\ 0 & -\eta\sin\psi & 0 & 0 & \cos\psi \end{bmatrix} \tag{38}$$

The Φ matrices for the remaining satellites are:

$$\Phi_i = \begin{bmatrix} 4-3\cos\psi & 0 & 0 & \frac{\sin\psi}{\eta} & \frac{2}{\eta}(1-\cos\psi) & 0 \\ -6(\sin\psi-\psi) & 1 & 0 & -\frac{2}{\eta}(\cos\psi-1) & -\frac{4}{\eta}\sin\psi+\frac{3\psi}{\eta} & 0 \\ 0 & 0 & \cos\psi & 0 & 0 & \frac{\sin\psi}{\eta} \\ 3\eta\sin\psi & 0 & 0 & \cos\psi & 2\sin\psi & 0 \\ 6\eta(\cos\psi-1) & 0 & 0 & -2\sin\psi & -3+4\cos\psi & 0 \\ 0 & 0 & -\eta\sin\psi & 0 & 0 & \cos\psi \end{bmatrix} \tag{39}$$

where the sign of components in the second row have been changed except for the y component due to the way Δy_i was defined.

The overall Φ matrix for this system has non-diagonal terms due to the interaction between the y coordinates of each satellite. The off-diagonal elements are:

$$\Phi_{i1} = \begin{bmatrix} 0 & 0 & 0 & 0 & 0 \\ 6(\sin\psi-\psi) & 0 & \frac{2}{\eta}(\cos\psi-1) & \frac{4}{\eta}\sin\psi-\frac{3\psi}{\eta} & 0 \\ 0 & 0 & 0 & 0 & 0 \\ 0 & 0 & 0 & 0 & 0 \\ 0 & 0 & 0 & 0 & 0 \\ 0 & 0 & 0 & 0 & 0 \end{bmatrix} \tag{40}$$

The overall system has the following form:

$$\hat{\mathbf{x}}(-) = \begin{bmatrix} \Phi_1 & 0 & \dots & 0 \\ \Phi_{21} & \Phi_2 & \dots & 0 \\ \vdots & \vdots & \ddots & \vdots \\ \Phi_{s1} & 0 & 0 & \Phi_s \end{bmatrix} \begin{bmatrix} \hat{x}_1(+) \\ \hat{x}_2(+) \\ \dots \\ \hat{x}_s(+) \end{bmatrix} = \Phi\, \hat{\mathbf{x}}(+) \tag{41}$$

The state is propagated from $t = 0$ to the desired δt before any updates are made, therefore the initial value for the state must be determined. The initial value for the estimated state $\hat{x}_0(t = 0)$ was set equal to the initial value from the truth model $x_t(t = 0)$ with the position measured in kilometers and the velocity measured in kilometers/second.

Once the state has been propagated through the first time interval, it must be updated. Since the measurements are discrete-time and nonlinear, the generic model for the measurements has the following form:

$$z(t_i) = h[x(t_i), t_i] + v(t_i) \tag{42}$$

where h is the filter's nonlinear estimate of the measurements and v is a white Gaussian noise sequence of zero mean and covariance of R_t which was described previously (4:40). This leads to the extended form of the Kalman filter update equation (4:44):

$$\hat{x}(+) = \hat{x}(-) + K\{z - h\,[\hat{x}(-)]\} \tag{43}$$

where K is the gain which will be determined once the covariance has been updated, and $h\,[\hat{x}(-)]$ is the filter's nonlinear estimate of the satellite's relative range before the state has been updated. The estimate of relative range has the following form:

$$h = \begin{bmatrix} \sqrt{(x_1 - x_2)^2 + \triangle y_2^2 + (z_1 - z_2)^2} \\ \vdots \\ \sqrt{(x_1 - x_s)^2 + \triangle y_s^2 + (z_1 - z_s)^2} \end{bmatrix} = \begin{bmatrix} h_1 \\ \vdots \\ h_{s-1} \end{bmatrix} \tag{44}$$

2.2.2 Covariance Propagation and Update .

In order to obtain numerical stability with single precision, the U-D covariance factorization version of the Kalman filter was used to propagate and update the covariance (3:392-399). This form of the filter was necessary to guarantee the positive semi-definiteness of the computed covariance matrix and to achieve numerical stability (8:2-15).

Double precision accuracy is obtained with single precision by factoring the covariance into two forms, the propagation of the covariance represented by $P(-)$ and the updating of the covariance represented by $P(+)$:

$$P(-) = U(-)\,D(-)\,U^T(-) \tag{45}$$

$$P(+) = U(+)\,D(+)\,U^T(+) \tag{46}$$

where the U matrix is upper triangular and unitary and the D matrix is diagonal.

The first step in the algorithm is to determine the initial values for the two matrices U and D by using the existing initial covariance P_0, which is a diagonal matrix. This initial covariance contains the steady state values determined from the initial testing accomplished by Captain Ward, which were 1×10^{-6} km for position and 1×10^{-12} $\frac{km}{sec}$ for velocity. This initial factorization is obtained using the following equations:

$$D_{nn} = P_{nn} \tag{47}$$

$$U_{in} = \begin{cases} 1 & i = n \\ P_{in}/D_{nn} & i = n-1,\, n-2,\, \ldots,\, 1 \end{cases} \tag{48}$$

where n represent the total number of states in the system $(6 * s - 1)$. As described previously, each satellite has six states except for satellite 1 which has five. The remaining columns in the matrices are computed as follows:

$$D_{jj} = P_{jj} - \sum_{k=j+1}^{n} D_{kk}\, U_{jk}^2 \tag{49}$$

$$U_{ij} = \begin{cases} 0 & i > j \\ 1 & i = j \\ \left[P_{ij} - \sum_{k=j-1}^{n} D_{kk}\, U_{ik}\, U_{jk}\right]/D_{jj} & i = j-1,\, j-2, \ldots, 1 \end{cases} \tag{50}$$

Now that the initial values have been determined, the covariance can be propagated to the first update time. Using the process above, the value for $U(+) = U_0$ and $D(+) = D_0$ have been determined and are used in forming two additional matrices. The first matrix is n-by-$2n$ and is designated as $Y(-)$:

$$Y(-) = [\mathbf{\Phi}\, \mathbf{U}(+) \mid \mathbf{G_d}] \tag{51}$$

where $\mathbf{\Phi}$ has been previously defined and $\mathbf{G_d}$ again is an identity matrix because the model is an equivalent discrete-time representation of a continuous-time system (3:337). The second matrix is a $2n$-by-$2n$ and is designated $\tilde{D}(-)$:

$$\tilde{D}(-) = \begin{bmatrix} D(+) & 0 \\ 0 & Q_d \end{bmatrix} \tag{52}$$

The propagation begins by transposing the $Y(-)$ matrix

$$Y^T(-) = [a_1\, a_2\, \ldots\, a_n] \tag{53}$$

and then calculating the following relationships for $k = n, n-1, \ldots, 1$

$$\begin{aligned}
c_k &= \tilde{D}(-)\, a_k \quad (c_{jk} = \tilde{D}_{jj}(-)\, a_{jk},\ j = 1, 2, \ldots, 2n) \\
D_{kk}(-) &= a_k^T\, c_k \\
d_k &= c_k / D_{kk}(-) \\
U_{jk}(-) &= a_j^T\, d_k \qquad\qquad j = 1, 2, \ldots\, k-1 \\
a_j &\leftarrow a_j - U_{jk}(-)\, a_k \quad j = 1, 2, \ldots, k-1
\end{aligned} \tag{54}$$

Now all the information has been calculated to propagate the covariance to the new time using Equation (45). The next step is to update the covariance. Several terms need to be defined for these calculations. Let the linearized measurement vector H_i be defined as:

$$H = \frac{\partial h}{\partial x}\,|_{x=\hat{x}(-)} \tag{55}$$

Using this definition the overall system **H** matrix has the following form:

$$\mathbf{H} = \begin{bmatrix} \tilde{H}_1 & H_1 & 0 & \ldots & 0 \\ \tilde{H}_2 & 0 & H_2 & \ldots & 0 \\ \vdots & \vdots & \vdots & \ddots & \vdots \\ \tilde{H}_{s-1} & 0 & 0 & \ldots & H_{s-1} \end{bmatrix} \tag{56}$$

where the individual matrices for $i = 1, 2, \ldots, s-1$ are defined as follows:

$$\tilde{H}_i = \left[\tfrac{x_i - x_{i+1}}{h_i} \quad \tfrac{x_i - x_{i+1}}{h_i} \quad 0 \quad 0 \quad 0 \right] \tag{57}$$

$$H_i = [-(\tfrac{x_1 - x_{i+1}}{h_i}) \quad \tfrac{\triangle y_{i+1}}{h_i} \quad -(\tfrac{x_i - x_{i+1}}{h_i}) \quad 0 \quad 0 \quad 0] \tag{58}$$

The H matrix is divided into individual row vectors and these are designated as H_i. The variable R_i is defined as the individual diagonal elements in the data covariance matrix R_f, which was assumed to be equal to R_t for this thesis. Now that all the terms have been defined the update can be computed. For $i = 1, 2, \ldots, s-1$

$$\begin{aligned} f &= U(-)^T H_i^T \\ v_j &= D_{jj}(-) f_j \qquad j = 1, 2, \ldots, n \\ a_0 &= R_i \end{aligned} \tag{59}$$

Then for $k = 1, 2, \ldots, n$

$$\begin{aligned} a_k &= a_{k-1} + f_k v_k \\ D_{kk}(+) &= D_{kk}(-) a_{k-1}/a_k \\ b_k &\leftarrow v_k \\ p_k &= -f_k / a_{k-1} \\ U_{jk}(+) &= U_{jk}(-) + b_j p_k \quad j = 1, 2, \ldots, (k-1) \\ b_j &\leftarrow b_j + U_{jk}(-) v_k \quad j = 1, 2, \ldots, (k-1) \end{aligned} \tag{60}$$

Using the values for $U(+)$ and $D(+)$ computed above the covariance can be updated using Equation (46). The gain of the filter is defined as:

$$K = \frac{b}{a_n} \tag{61}$$

with b composed of the most resent components calculated in Equation (60). The

state update can now be determined using Equation (43). This entire process of propagating and updating the state and covariance is repeated at a time interval specified by the user until a final time is reached.

In summary, this chapter developed the truth model based on the two-body equations of motion. This model consisted of the relative position and velocity components of each satellite with respect to a rotating reference point. A U-D covariance factorization version of the Kalman filter was used to determine the estimated position and velocity of each satellite using the measurement data provided by the truth model. A modification to the y component of both the truth model and filter became necessary due to observability problems. The modification included replacing the absolute y_i component of satellite $2-s$, with a relative $\triangle y_i$ component by removing the y component from satellite 1. The state for satellite 1 was reduced to five components with the other members of the cluster retaining six components. The next step will be to test the filter.

III. Initial Testing

Now that the true state and estimated state have been computed, the true error e_t of the position components can be obtained. The errors in the velocity will not be computed since the purpose of this thesis is to determine the accuracy of the filter's estimate of the relative position of each satellite in the cluster. The error in the velocity will cause the filter's computed cluster to separate and this separation will appear as errors in the position components. Since the elements of the true state and estimated state are of the same type, for $i = 1, 2, 3, \ldots, s$ the true error is defined as:

$$e_t = \left[(\hat{x}_i - x_{t_i})^2 + (\hat{y}_i - y_{t_i})^2 + (\hat{z}_i - z_{t_i})^2\right]^{\frac{1}{2}} \tag{62}$$

where the $(\hat{y}_i - y_{ti})^2$ component is missing for satellite 1. Once the true error has been computed it can be compared to the estimated error which is defined as the average standard deviation of the position components computed from the covariance, which again is a measure of how well the filter thinks it is performing. The estimated error is computed using the following equation:

$$\sigma_{avg} = \sqrt{\sigma_x^2 + \sigma_y^2 + \sigma_z^2} \tag{63}$$

where $\sigma^2_{x,y,z}$ are the eigenvalues of the position covariance matrix. For Captain Ward's thesis the true error was compared to the maximum standard deviation (σ_{max}) of the covariance, which was defined as the square root of the largest eigenvalue of the position covariance matrix. The comparison was changed initially in a attempt to determine if the curves for the true error could be made to match the average values of the covariance position components to a higher degree. This assumed that the filter was performing properly, which was later discovered to be untrue. Any

further investigations into this problem should revert back to a comparison of the maximum standard deviation.

3.1 Sample Runs

Captain Ward tested the filter's accuracy by accomplishing single performance runs, which involve using only one seed value in the random number generator. During the runs, the number of satellites in the cluster was varied and different values of dynamics driving noise covariance Q_d were used to tune the filter. The filter's relative measurement covariance R_f was equal to R_t for all time and was based on an assumed range error of .01 meters. The cluster radius was 500 meters at a reference altitude of 1000 kilometers above the earth with an orbital period of approximately 6300 seconds (8:3-2-3-3).

Initially the filter's stability was verified by Captain Ward, and runs were conducted to determine if the true error was within the required accuracy. The filter performed within the desired accuracy in all cases, including the addition of noisy data to the estimator. The maximum transient response of the estimated error was periodic with a peak at every half of an orbit of approximately 2 meters and the maximum value of the true error, which was also periodic, was approximately .01 meters for satellite 1 and close to zero for the other satellites. When noise was added to the data, the true error as expected, increased to around .5 meters and in the case of satellite 1 this error grew to exceed the filter's computed error statistics (σ). Through the addition of more dynamics noise in the tuning of the filter, the true error decreased to a value below the filter's estimated error. The first task of this thesis was to verify the results obtained by Captain Ward. The code was obtained and it was determined that it had been developed and run on a Digital Equipment Corporation VAX-11-785 with a VMS operating system. The code ran without incident, but the results obtained were not the same as the Ward thesis. The results of satellite 1 showed the largest deviation with large peaks in the true error occurring in the

initial test run which contained only two satellites and no driving noise covariance Q_d. Since the Ward thesis did not specify an update time, the code was rerun with updates every 1 minute. The results still did not change. At this point it was assumed this was not the latest version of the code. Since the state of satellite 1 was decreased to five states in the last version of the filter, this investigation searched for errors in the computation of the estimated state for satellite 1. This proved to be the problem. The computation of the true error for satellite 1 was accounting for three position components, not two. Several small errors were also found in the computation of the initial values for the U_0 and D_0 matrices and several matrices whose values were computed in the filter were initialized to zero to insure their values. Later in the testing it was discovered that during the measurement update, the components of the $U(-)$ matrix were being updated with each measurement, but components of the $U(-)^T$ matrix were not. This made no difference with two satellites in the cluster, but it made a large difference with 10 satellites by further decreasing the true error. With the above changes, several of the cases presented in the Ward thesis were validated with single performance runs containing perfect data and were then followed by a full Monte Carlo analysis. The set-up for the Monte Carlo analysis will be presented in more detail later in this section.

The first test of the filter was a stability analysis. The cluster contained two satellites, with the dynamics driving noise matrix Q_d entries equal to zero. The resulting graph, Figure 5, shows a well behaved filter with the filter's estimated error decreasing and the initial true error equal to zero. The true error, as expected, began to diverge once it had reached a near zero value because the filter assumed it had reached perfection and ignored the new measurement data coming in. This was a result of an inappropriate choice of $Q_d = 0$.

The next test was to add driving noise to prevent the filter from locking onto a state and ignoring the measurement data. The initial conditions used above were rerun to match the Ward thesis with the Q_d matrix entries set equal to 1×10^{-12} km

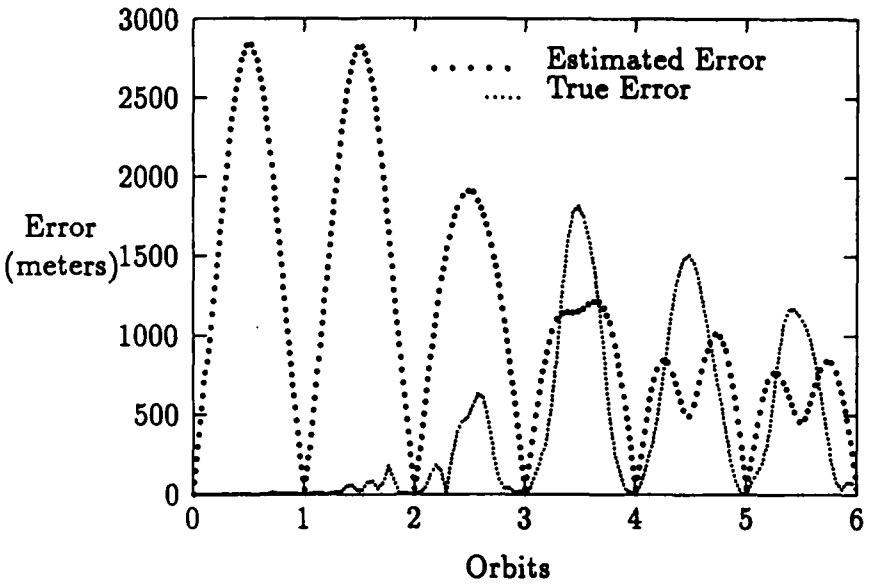

Figure 5. Stability Analysis

for position and 1×10^{-17} $\frac{km}{sec}$ for velocity. Figure 6, shows the true error is still diverging but at a slower rate, as expected. The values chosen for the Q_d matrix were apparently not large enough.

The addition of more satellites to the cluster was the next test to determine if additional measurements would improve the true error. The cluster size was increased to five satellites with all other parameters remaining constant. This again improved the true error, but unlike the results of the Ward thesis, the estimated error in Figure 7 did not not lock onto a state and converge to zero.

The final test was to increase the cluster to the maximum of 10 satellites, with the initial covariance matrix entries set equal to their steady state values of 1×10^{-6} km for position and 1×10^{-12} $\frac{km}{sec}$ for velocity. Since the filter seemed to be tuning with the addition of less driving noise, the entries of the Q_d matrix were decrease from 2×10^{-9} km to 1×10^{-10} km for position and from 2×10^{-14} $\frac{km}{sec}$ to 1×10^{-15} $\frac{km}{sec}$ for velocity.

Figures 8 and 9 show the true error is no longer diverging, but the filter is still

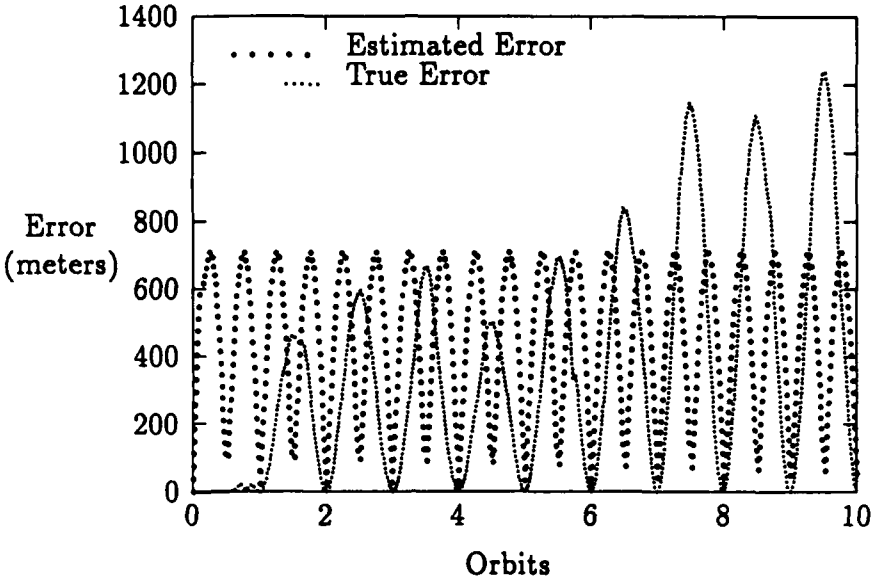

Figure 6. Satellite One of Two with Driving Noise

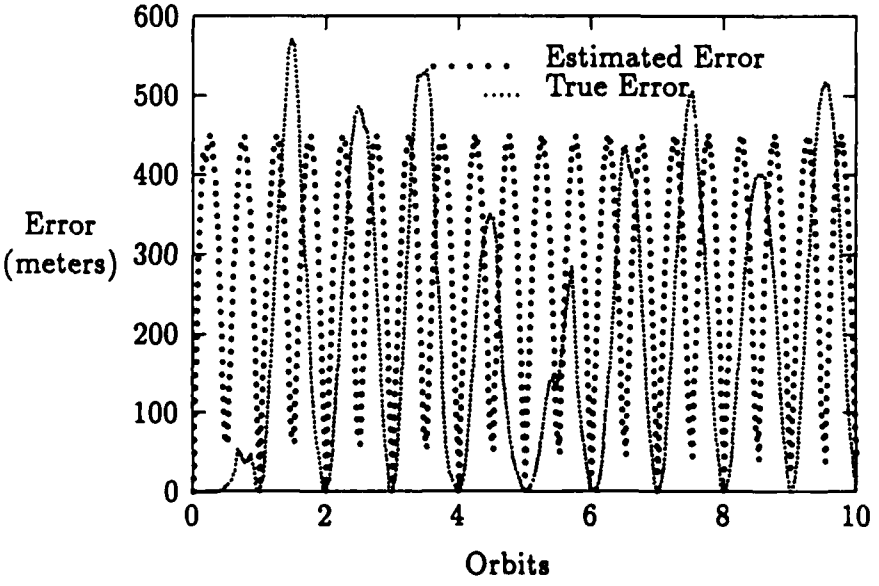

Figure 7. Satellite One of Five with Driving Noise

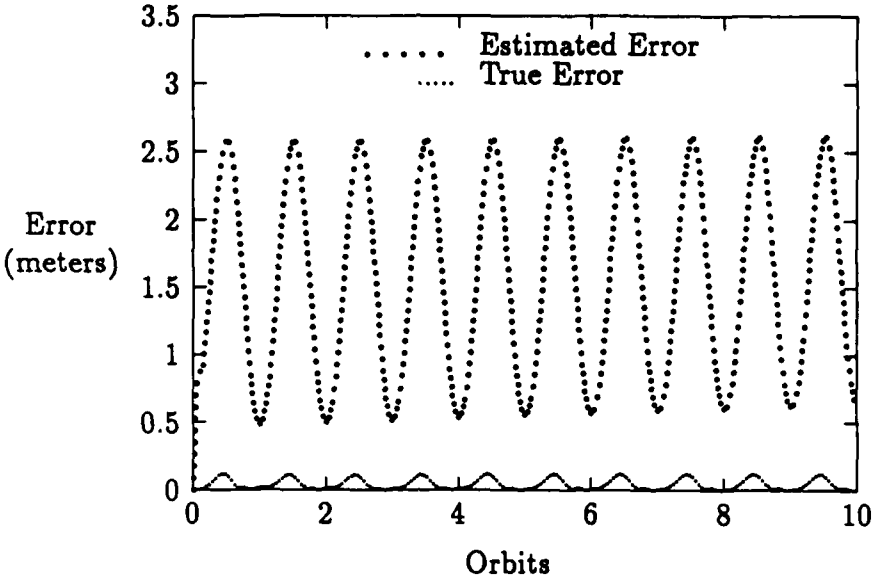

Figure 8. Satellite One with Steady-State Covariance and Driving Noise

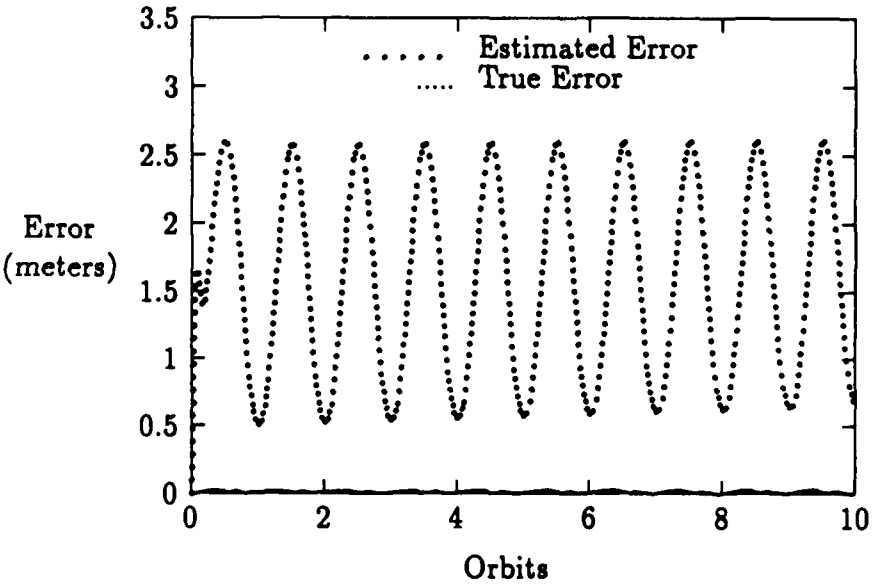

Figure 9. Satellite Ten with Steady-State Covariance and Driving Noise

overestimating its own error. The graphs also show the error for satellite 1 differs from that of the other satellites. This was also discovered in the Ward thesis. The apparent explanation lies in the difference between the number of components in the state vector for satellite 1 and the other members of the cluster.

With the code running properly, the program was transferred to another computer in order to speed computation time for the Monte Carlo simulation. The code was put on an Elxsi Superframe with an EMBOS operating system and running an EMS VMS operating system emulator. The code was changed in several areas to account for system architectural differences. One obvious difference in the machine architecture was the number of digits carried by the machine for single precision which is used in the calculations of the estimated states. The VAX carried twelve digits and the Elxsi carries only nine. Since the error between the true state and the estimated state was approximately .1 meters, this difference did not effect the results. When the code was tested on the new computer, the results matched those previously obtained with a the running time reduced from 30 minutes for a case with ten satellites to six minutes.

The next step was to test the filter in a full Monte Carlo simulation. The simulation was conducted by varying the seed values used by the random number generator to determine the placement of satellites around the reference point. Ten different seed values were used and runs were completed with each of these seed values. The outputs were then averaged together to obtain the final results. The average true error and average estimated error were computed as follows:

$$\textit{average true error at each time interval} = \sum_{k=1}^{n} \frac{\sum_{i=1}^{10}(\hat{x}_i(k) - x_{ti}(k))}{10} \qquad (64)$$

where k represents each element in the state vector and i represents the value computed for each element at that time interval, and

$$average\ variance\ at\ each\ time\ interval = \sum_{i=1}^{10} \frac{\sqrt{\sigma(x_i)^2 + \sigma(y_i)^2 + \sigma(z_i)^2}}{10.0} \qquad (65)$$

where again the $\sigma^2_{x,y,z}$ values are the eigenvalues of the position covariance matrix. The results of the simulation, Figures 10 and 11, show the same pattern as the single sample case.

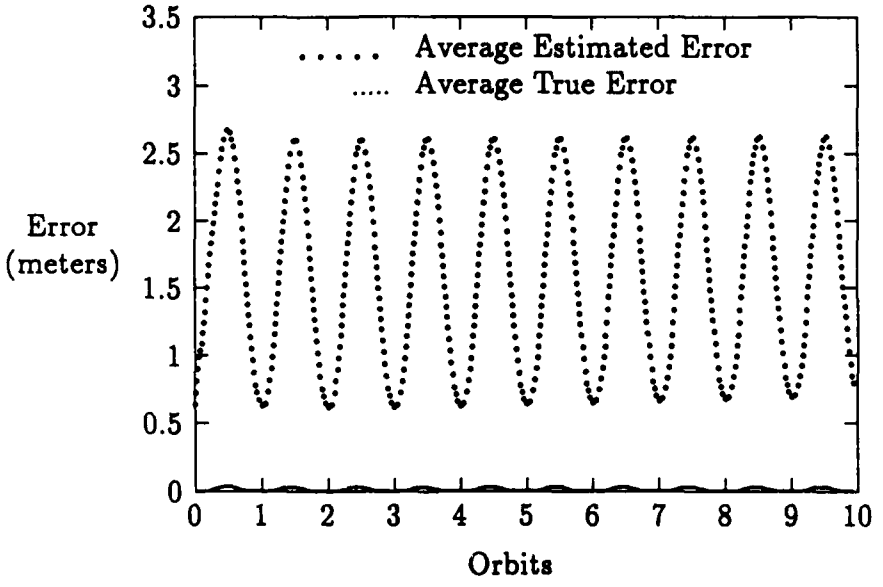

Figure 10. Satellite One's Averaged Performance

The next step in the testing of the filter was the addition of noisy data to the system. The data error standard deviation was initially set at .01 meters and the driving noise entries were set equal to 2×10^{-9} km for position and 2×10^{-14} $\frac{km}{sec}$ for velocity.

Figure 12 shows there is too much driving noise in the system which is causing the filter's computed error to diverge from the true error. Through additional testing the estimated error converged when the driving noise entries were decreased to 1×10^{-12} km for position and 1×10^{-17} $\frac{km}{sec}$ for velocity. The amount of noise in the

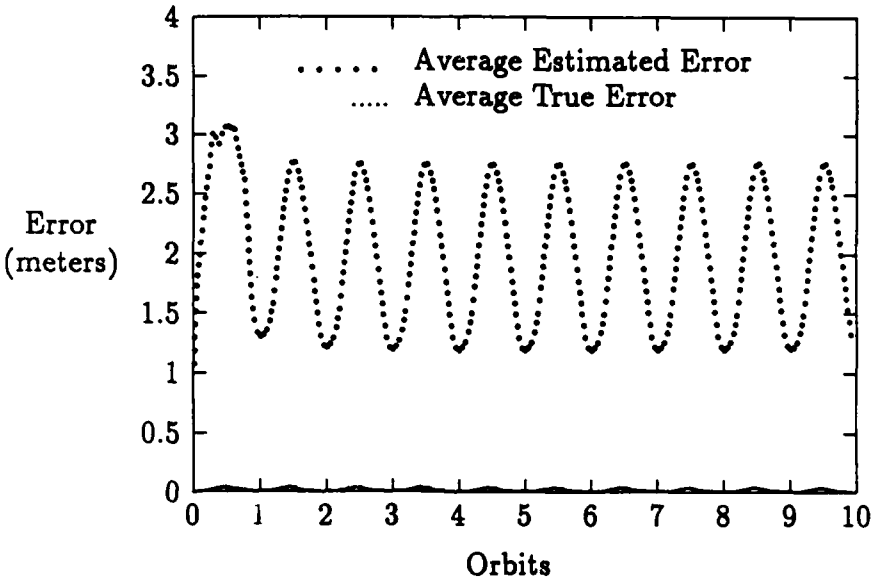

Figure 11. Satellite Ten's Averaged Performance

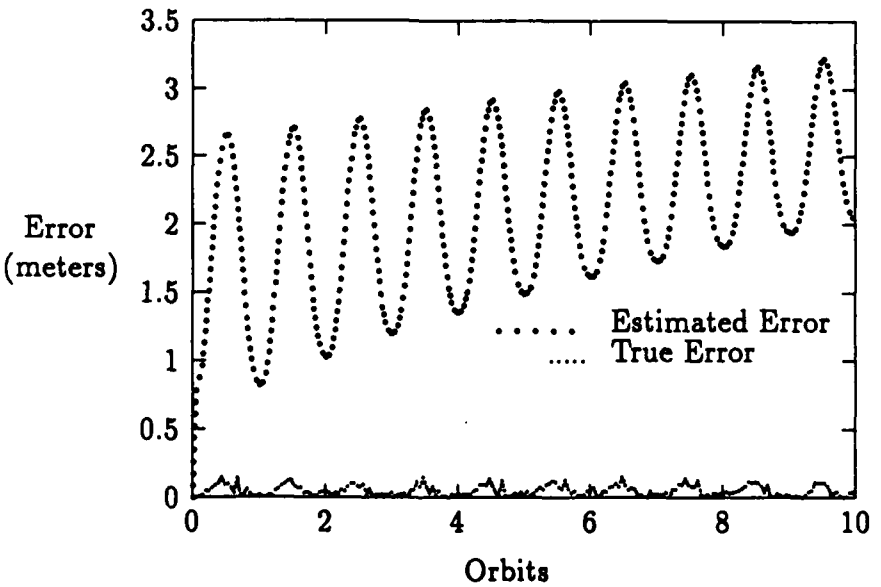

Figure 12. Satellite One of Ten with .01 Meter Noisy Data

data was also increased to a standard deviation of one meter to insure that the data covariance in single precision was not zero *km*. The resulting graphs, Figures 13 and 14, show the estimated error is no longer diverging, but the true error is still too large.

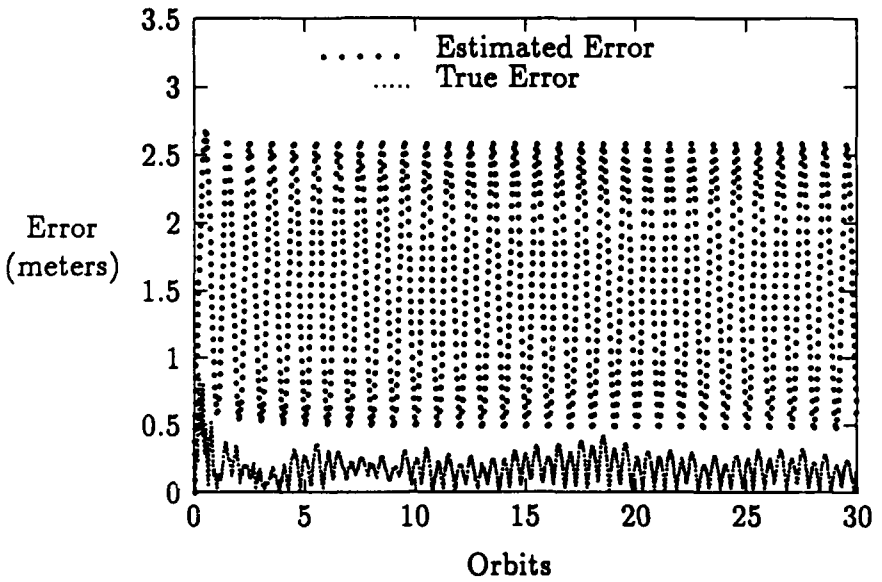

Figure 13. Satellite One of Ten with 1 Meter Noisy Data

Another method of decreasing the true error is by updating the filter at smaller time intervals. The update cycle was decreased from once every five minutes to once every three minutes. As expected, Figures 15 and 16 show that the true error has decreased to a more acceptable level, but the filter is still poorly tuned.

Before a Monte Carlo simulation was run for the case with noisy data, the inability of the estimated error to converge to the true error and the increased true error in the case of satellite 1, were investigated. The desired response of the filter would be for the true error to match the filter's estimate of the error. The filter's computed error in the above runs stays periodic and seems to be unable to match the value of the true error with the information provided. A hypothesis for the cause of this limit and the increased true error for satellite 1, is the inability of the filter

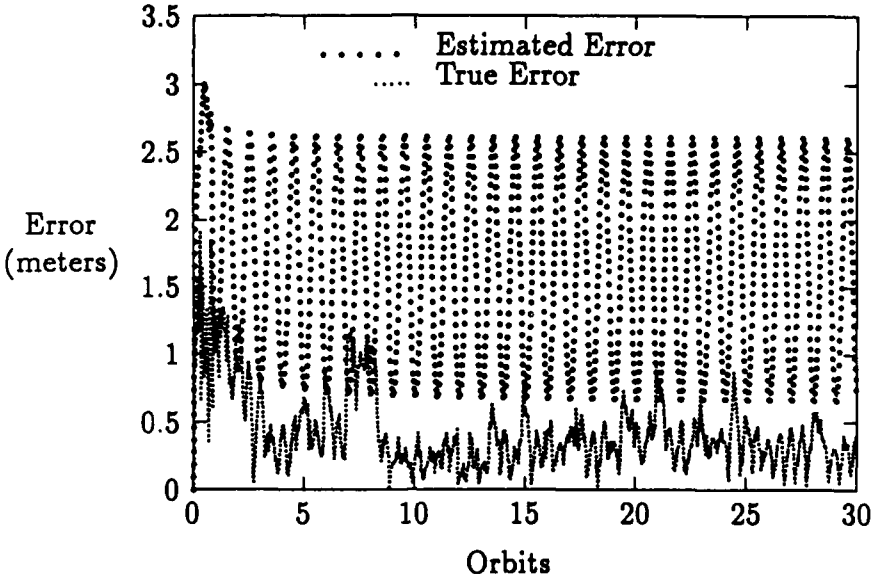

Figure 14. Satellite Ten of Ten with 1 Meter Noisy Data

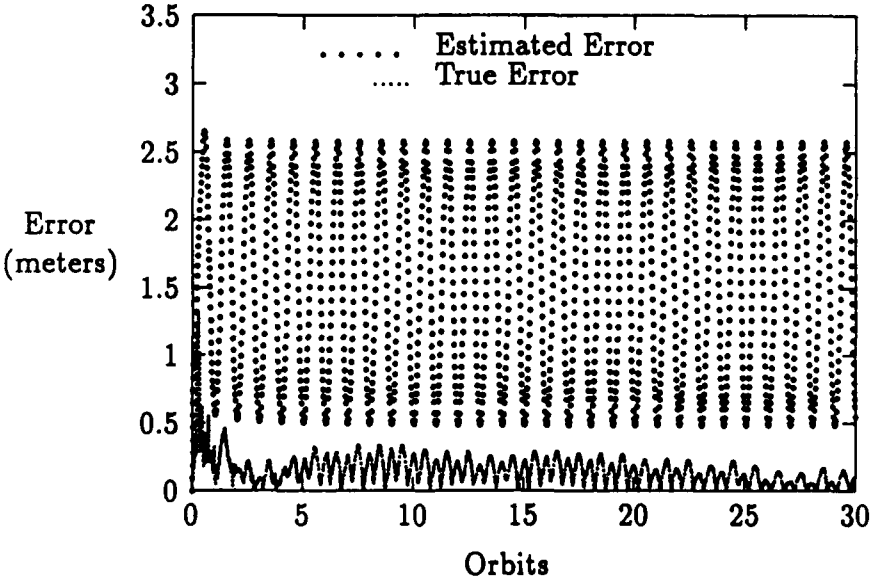

Figure 15. Satellite One with Three Minute Updates

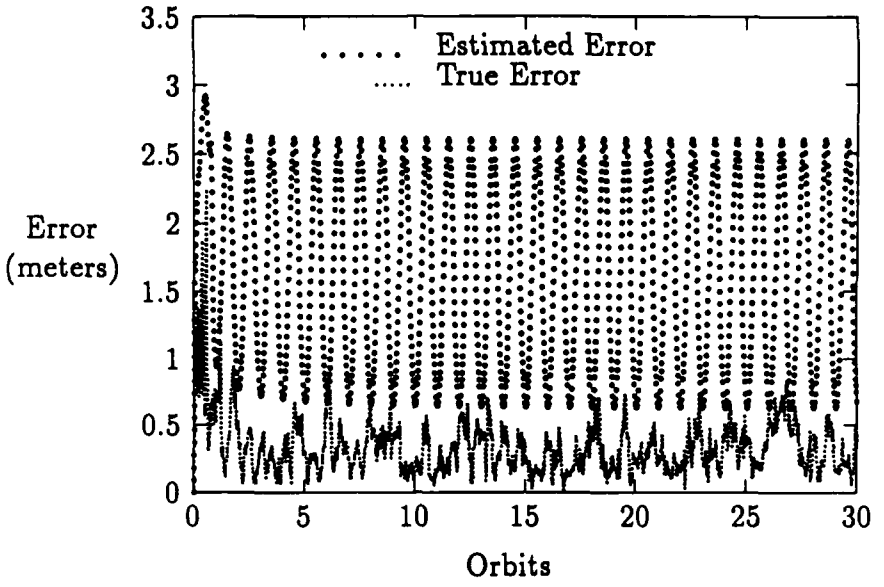

Figure 16. Satellite Ten with Three Minute Updates

to observe a necessary state from the measurements available. The hypothesis was tested by using the Kalman filters resident on each satellite in the cluster to feed their measurement data back to satellite 1 for use in the update computation. In this manner the filter on satellite 1 will have additional data on which to base its estimate.

The purpose of this chapter was to validate the results achieved by Ward. The cases presented in the Ward thesis were rerun, but due to a small error in the measurement update cycle, the results did not match those previously obtained. The results obtained in this chapter show that the true error has improved over that obtained by Ward and requires smaller values for the driving noise entries to keep from diverging. The filter's computed error has not followed this improvement causing the filter to be poorly tuned. The next step is to investigate further this observability or observability-like problem.

IV. Additional Data and Observability Test

4.1 Additional Filters

One method of obtaining additional data is to use the Kalman filter described previously on every satellite in the cluster. Then at each time interval, satellite 2 through s would send all of their measurement data to satellite 1 for inclusion in the computation of the total estimated state and the position covariance. Satellite 1 would determine which satellite was providing the measurements. The variable used in the calculations to determine which satellite was currently providing measurement data as well as a clock pulse to satellite 1 was termed *view*. For $view = 1, 2, 3, \ldots, s-1$ the linearized measurement matrix becomes

$$h = \begin{bmatrix} \sqrt{(x_{view} - x_{view+1})^2 + (\triangle y_{view+1})^2 + (z_{view} - z_{view+1})^2} \\ \cdots \\ \sqrt{((x_{view} - x_s)^2 + (\triangle y_s^2) + (z_{view} - z_s)^2} \end{bmatrix} = \begin{bmatrix} h_{view} \\ \cdots \\ h_{s-view} \end{bmatrix} \quad (66)$$

In order to avoid duplication of data, the number of measurements sent to satellite 1 would decrease with each additional satellite present in the cluster. For example, if there were four satellites in the cluster, satellite 1 would update the state with clock pulses from satellite two, three, and four, satellite 2 would provide measurement data to satellite 1 from the clock pulses it received from satellites three and four, and finally satellite three would provide measurement data from the clock pulse it received from satellite four. The maximum number of measurements available for a ten satellite cluster is 55.

The entire linearizaton measurement matrix will also vary depending on the satellite that is providing the measurement data. For satellite 1, recall the overall matrix appears as follows:

$$\mathbf{H} = \begin{bmatrix} \tilde{H}_1 & H_1 & 0 & \dots & 0 \\ \tilde{H}_2 & 0 & H_2 & \dots & 0 \\ \vdots & \vdots & \vdots & \ddots & \vdots \\ \tilde{H}_{s-1} & 0 & 0 & \dots & H_{s-1} \end{bmatrix} \tag{67}$$

When the satellite providing the measurements changes, this matrix remains the same size coming into satellite 1 by using zeros as place holders. For measurements from satellite 2 the matrix would appear as follows:

$$\mathbf{H} = \begin{bmatrix} 0 & 0 & 0 & 0 & \dots & 0 \\ 0 & \tilde{H}_2 & H_2 & 0 & \dots & 0 \\ 0 & \tilde{H}_3 & 0 & H_3 & \dots & 0 \\ 0 & \dots & \dots & \dots & \ddots & \dots \\ 0 & \tilde{H}_{s-2} & 0 & 0 & \dots & H_{s-2} \end{bmatrix} \tag{68}$$

where for $i = 2, 3, \dots, s-1$

$$\tilde{H}_i = \begin{bmatrix} \frac{x_2 - x_{i+1}}{h_i} & \frac{z_2 - z_{i+1}}{h_i} & 0 & 0 & 0 \end{bmatrix} \tag{69}$$

$$H_i = \begin{bmatrix} -\frac{(x_2 - x_{i+1})}{h_i} & \frac{\Delta y_{i+1}}{h_i} & -\frac{(z_2 - z_{i+1})}{h_i} & 0 & 0 & 0 \end{bmatrix} \tag{70}$$

The filter on satellite $2, 3, 4, ..., s$ would have the same values as satellite 1 for the initial covariance matrix P_0, and driving noise matrix covariance Q_d. Each of these filters would run independently, but send their measurement data to satellite 1 besides using the data to update their own estimate. The state vectors on each satellite would also mimic the state vector for satellite 1 by having only five elements in the state vector for the number corresponding to the satellite. For example, the filter on satellite 2 would have the following overall state vector components for $i = 3, 4, .., s$:

$$x_2 = \begin{bmatrix} x_2 \\ z_2 \\ \dot{x}_2 \\ \dot{y}_2 \\ \dot{z}_2 \end{bmatrix} \quad and \; x_i = \begin{bmatrix} x_i \\ \Delta y_i \\ z_i \\ \dot{x}_i \\ \dot{y}_i \\ \dot{z}_i \end{bmatrix} \tag{71}$$

The initial testing of this new system was the placement of filters on satellites 1 and 2 in a three satellite cluster. The initial conditions were the same as those in Figure 8. The resulting graphs, Figure 17 and Figure 18, show the filter's estimated error has increased and it is still unable to match the true error. The additional data had no effect on the true error for satellite 1.

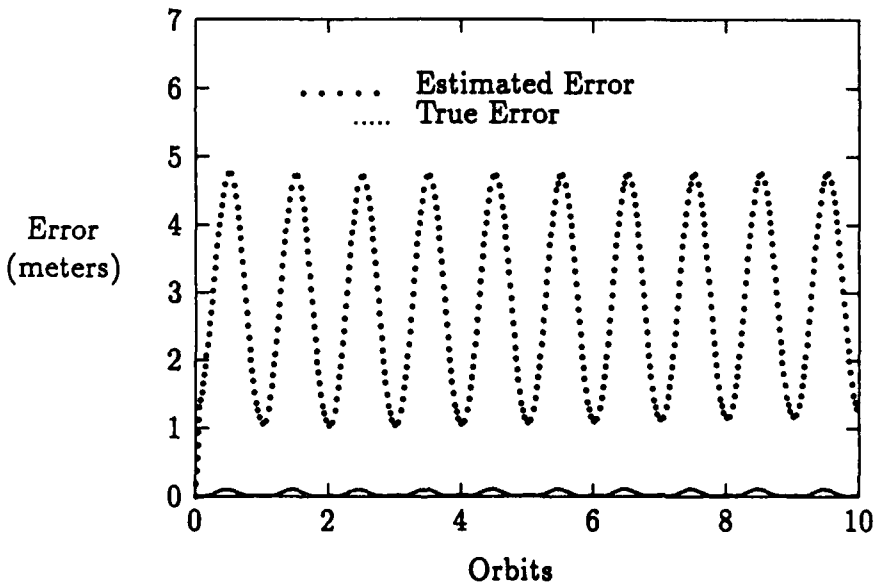

Figure 17. Satellite One with Measurements from Satellites One and Two

The additional measurements provided to satellite 1 do not directly update satellite one's components; they work by allow the filter to determine where the other satellites in the cluster are to a higher degree and thereby allowing satellite 1

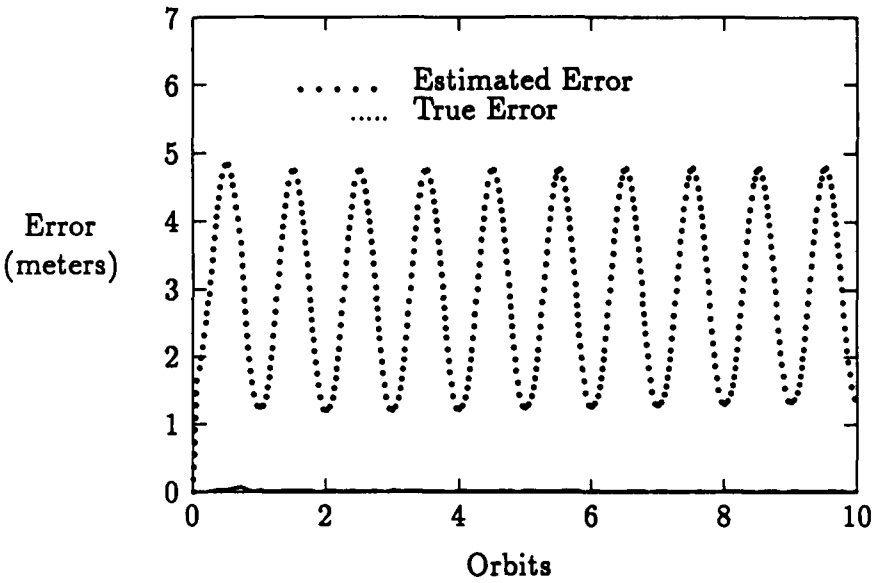

Figure 18. Satellite Three with Measurements from Satellites One and Two

to determine its position to a higher degree. Figure 17 and Figure 18 demonstrate that this approach does not seem to be solving the problem. The next step was to look at the filter on satellite 2 and determine its performance. The filter on this satellite demonstrated the same pattern as that seen with satellite 1 by not being able to lock onto its own state to the same degree that it locks onto other members of the cluster. This would seem to give credence to the statement that the change in the true error is due to the difference in the number of elements in the state vector between the satellite the active filter is residing and the other satellites in the cluster.

In order to determine what information the measurements were providing to the filter, the value of each state position component error was plotted against this same error after the last update of that time interval for a one filter system. The component error is defined as:

$$e = \begin{bmatrix} (\hat{x} - x_t) \\ \Delta y_i \\ (\hat{z} - z_t) \end{bmatrix} \tag{72}$$

Figure 19 and Figure 20 show the results of this test for satellite 1 in a ten satellite cluster. The graphs show the value of the error changes very little after the update and in some cases the error after the update has increased.

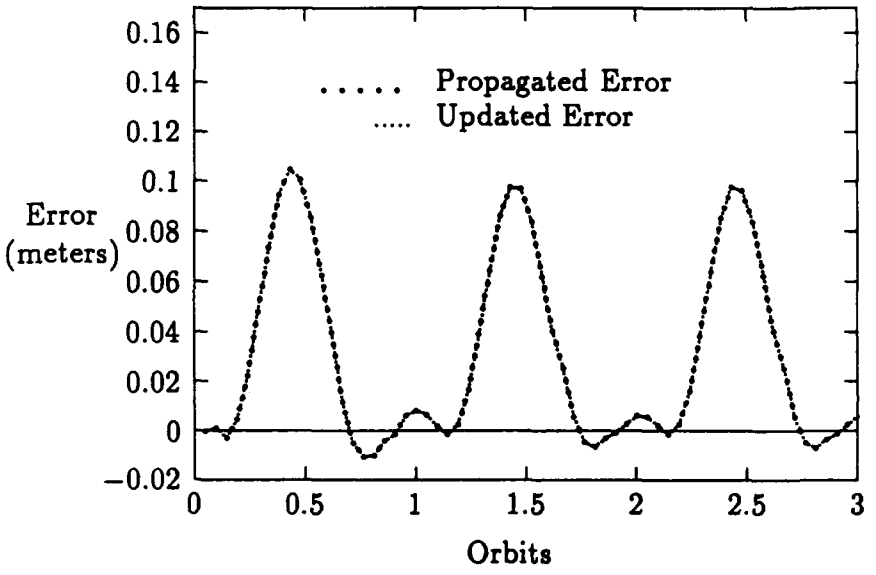

Figure 19. Estimated Minus True x Component Values

This same test was performed for satellite 2. The resulting graphs, Figure 21 and Figure 22, show the value of the component error is decreasing after the update as expected.

All of the other members of the cluster showed results similar to those of satellite 2. The value of the gain was checked to insure it was not zero and thereby not allowing satellite 1 to update. The opposite situation was found. The update values for the components of satellite 1 are higher than the update values for satellite 2. Since the value of the filter's internally computed state component is initially

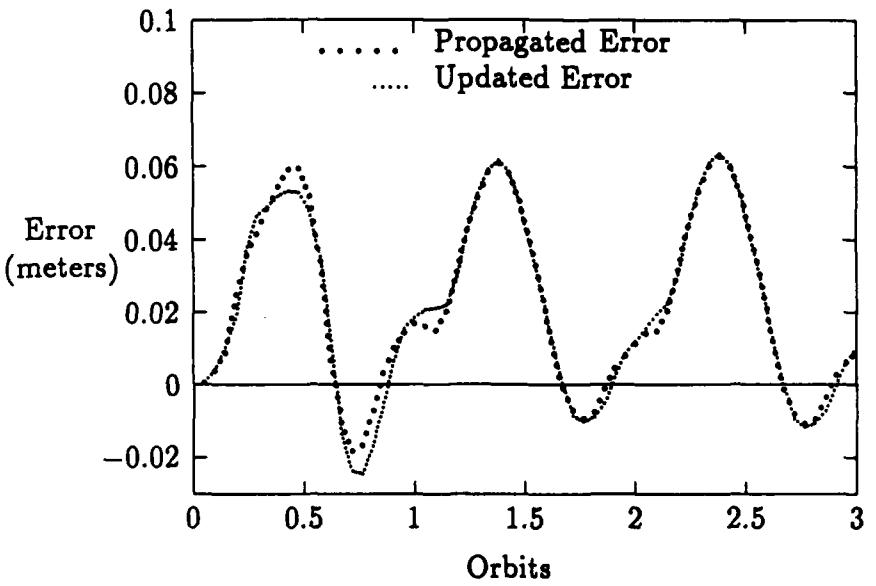

Figure 20. Estimated Minus True z Component Values for Satellite One

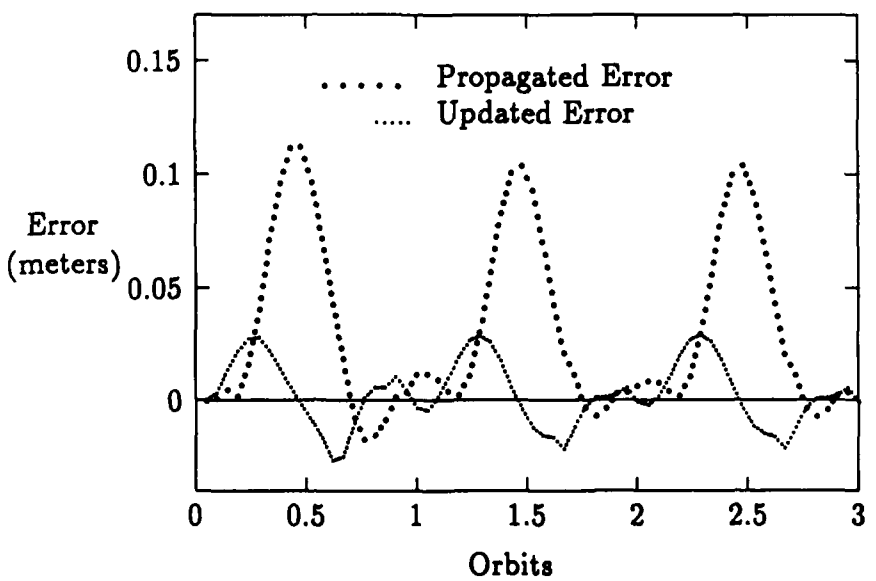

Figure 21. Estimated Minus True x Component Values for Satellite Two

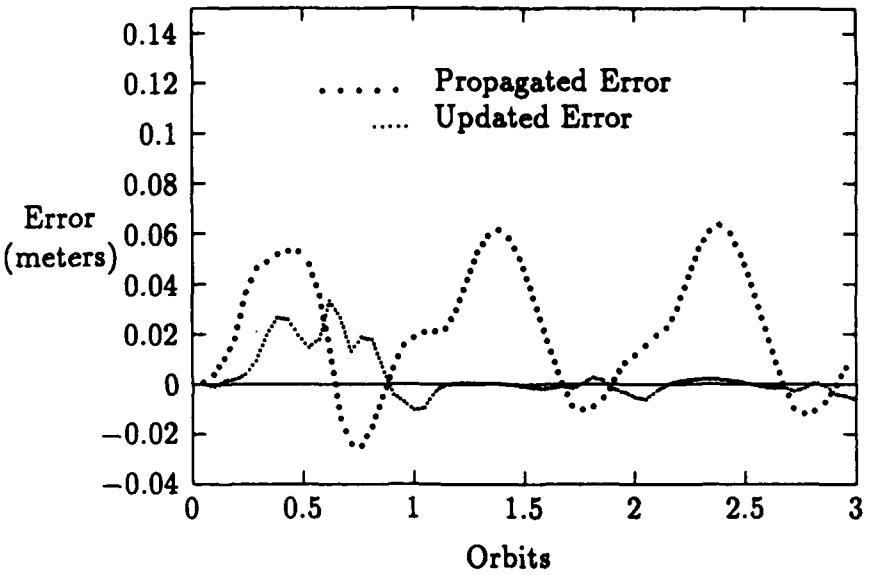

Figure 22. Estimated Minus True z Component Values for Satellite Two

greater than the component value from the truth model, the greater update value is actually increasing the error in the component rather than decreasing it. The value of the update can be lowered by decreasing the initial value of the covariance P_0 for satellite 1, which in turn decreases the gain. With the initial entries for the position covariance decreased from 1×10^{-6} km to 1×10^{-17} km the case was rerun. The results show the gain decreased slightly for one period but then returned to its original pattern. One possible explanation for these results is that another component in satellite one's state vector is unobservable.

4.2 Observability

The inability of the estimated $\hat{z}$ and $\hat{x}$ components of satellite 1 to update suggests that the z and $\dot{z}$ components of each satellites state vector may be unobservable, along with a component used in the propagation of $\hat{x}$ component. The first test was to remove the z, $\dot{z}$ and $\dot{y}$ components from satellite one's state vector and replace these components in satellites $2-s$ with their relative components. The same

steps that were used to remove the y component from the system were repeated. For $i = 2, 3, ..., s$

$$\triangle z = z_1 - z_i \tag{73}$$

$$\triangle \dot{y} = \dot{y}_1 - \dot{y}_i \tag{74}$$

$$\triangle \dot{z} = \dot{z}_1 - \dot{z}_i \tag{75}$$

For $i = 1, 2, 3, ..., s$, the new state vectors appear as follows:

$$x_1 = \begin{bmatrix} x_1 \\ \dot{x}_i \end{bmatrix} \; and \; x_i = \begin{bmatrix} x_i \\ \triangle y_i \\ \triangle z_i \\ \dot{x}_i \\ \triangle \dot{y}_i \\ \triangle \dot{z} \end{bmatrix} \tag{76}$$

The Φ matrix for satellite 1 was reduced to a 2-by-2 matrix:

$$\Phi_1 = \begin{bmatrix} 4 - 3\cos\psi & \frac{\sin\psi}{\eta} \\ 3\eta\sin\psi & \cos\psi \end{bmatrix} \tag{77}$$

The Φ matrix for satellite i, where $i = 2, 3, ..., s$ remains a 6-by-6 matrix with the sign of the x and $\dot{x}$ components changed is:

$$\Phi_i = \begin{bmatrix} -4+3\cos\psi & 0 & 0 & -\frac{\sin\psi}{\eta} & \frac{2}{\eta}(1-\cos\psi) & 0 \\ -6(\sin\psi-\psi) & 1 & 0 & -\frac{2}{\eta}(\cos\psi-1) & \frac{4}{\eta}\sin\psi-\frac{3\psi}{\eta} & 0 \\ 0 & 0 & \cos\psi & 0 & 0 & \frac{\sin\psi}{\eta} \\ -3\eta\sin\psi & 0 & 0 & -\cos\psi & 2\sin\psi & 0 \\ -6\eta(\cos\psi-1) & 0 & 0 & 2\sin\psi & -3+4\cos\psi & 0 \\ 0 & 0 & -\eta\sin\psi & 0 & 0 & \cos\psi \end{bmatrix} \quad (78)$$

where again ψ is $\eta\delta t$, and δt is the sampling time. The off-diagonal matrix Φ_{i1} has additional terms due to the removal of $\dot{y}$ term.

$$\Phi_{i1} = \begin{bmatrix} 0 & 0 \\ 6(\sin\psi-\psi) & \frac{2}{\eta}(\cos\psi-1) \\ 0 & 0 \\ 0 & 0 \\ 6\eta(\cos\psi-1) & -2\sin\psi \\ 0 & 0 \end{bmatrix} \quad (79)$$

The overall Φ matrix has the same form that was presented previously with the Φ_1 and Φ_{i1} matrices reduced from 5-by-5 and 6-by-5 to 2-by-2 and 6-by-2 matrices respectively.

This system of state components was tested with the same conditions as those present in Figure 8. The resulting graphs, Figure 23 and Figure 24, show a large increase in the true error for all of the states. The filter's estimated error has remained very small and is represented by the dark line at the bottom of the graphs.

Since the state vector for satellite 1 contains only the x position component and still contains large values for the true error, the most likely cause of the large error was the removal of the $\dot{y}$ component from the state vectors. This was shown even more clearly when the $\dot{y}$ component was put back into the propagation of $\hat{x}$ and

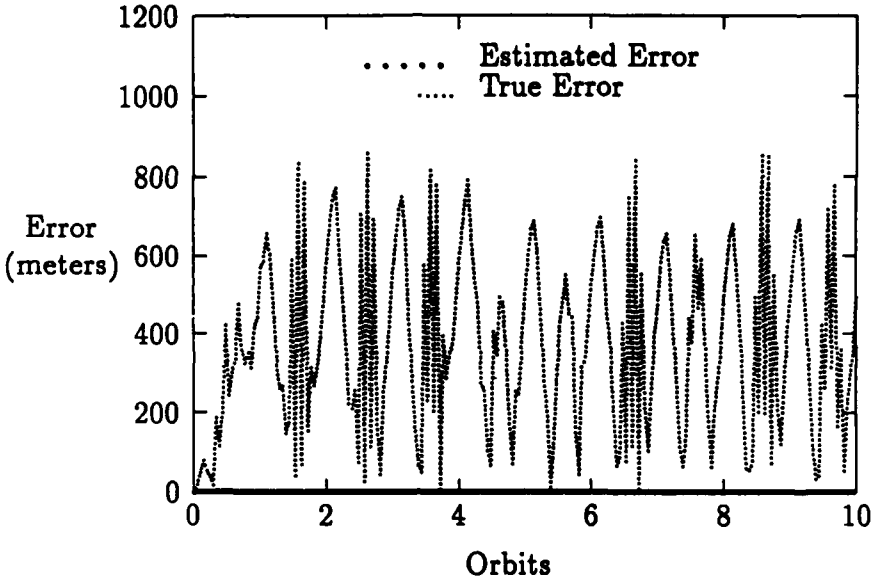

Figure 23. Satellite One with $y, z, \dot{y}$ and $\dot{z}$ Missing

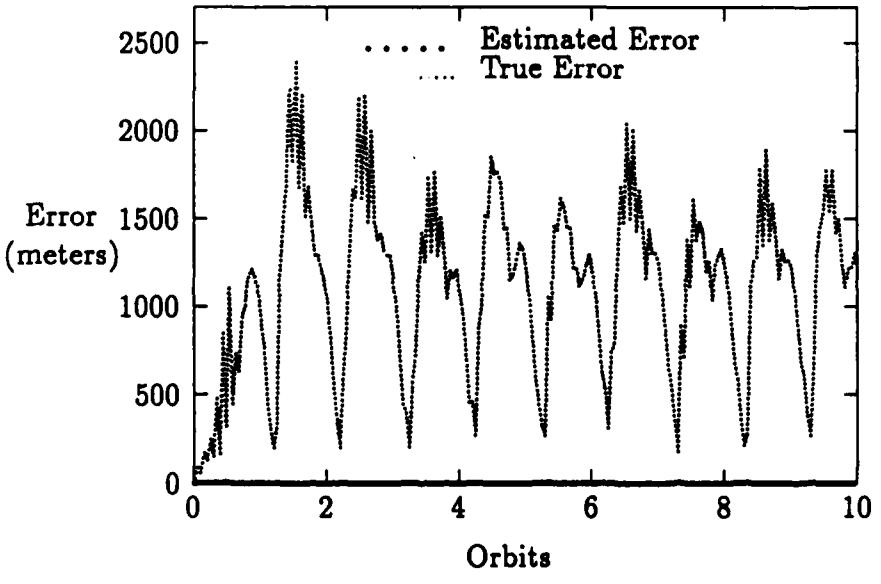

Figure 24. Satellite Ten Error with $y, z, \dot{y}$ and $\dot{z}$ Missing

just the z and $\dot{z}$ components of the state vector were removed. The resulting graphs Figure 25 and Figure 26, show satellite 1 still has the error in the x component of its state vector and the periodic estimated error since it is not updating and being affected by the noisy data. The results for satellites $2-s$ are closer to those obtained with the z and $\dot{z}$ components remaining, but their removal has not improved the filter's performance.

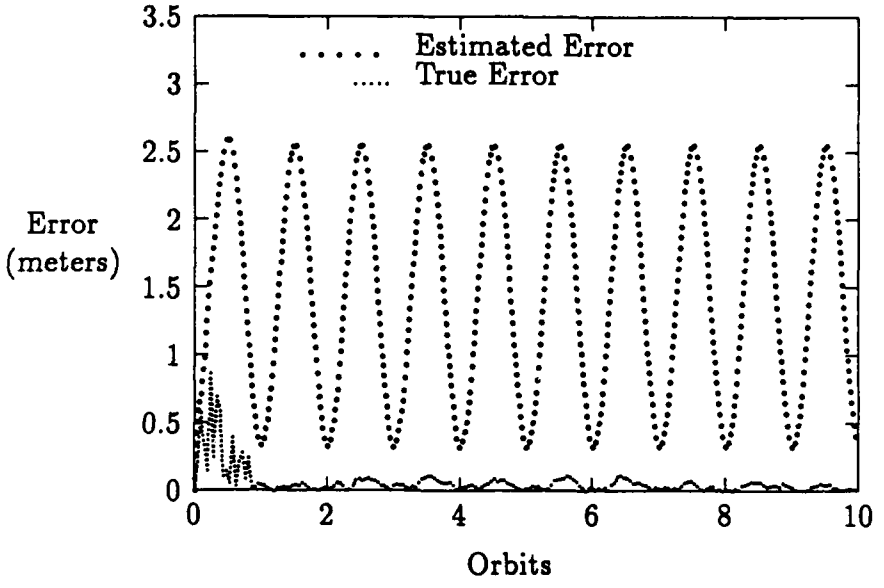

Figure 25. Satellite One Error with z and $\dot{z}$ Components Removed

Several other combinations of states revealed quickly that the y component is the only state that is obviously unobservable. Since the error in the system depends on the position in the orbit, the error defined as the estimated state minus the true state of the system was computed by propagating the state vectors back to $t = 0$ after every propagation interval. The state is propagated backward in time by using the inverse of the Φ matrix in the following manner:

$$x_0(+) = \sum_{i=1}^{\frac{t}{\delta t}} \Phi^{-1} \mathbf{x}(+) \tag{80}$$

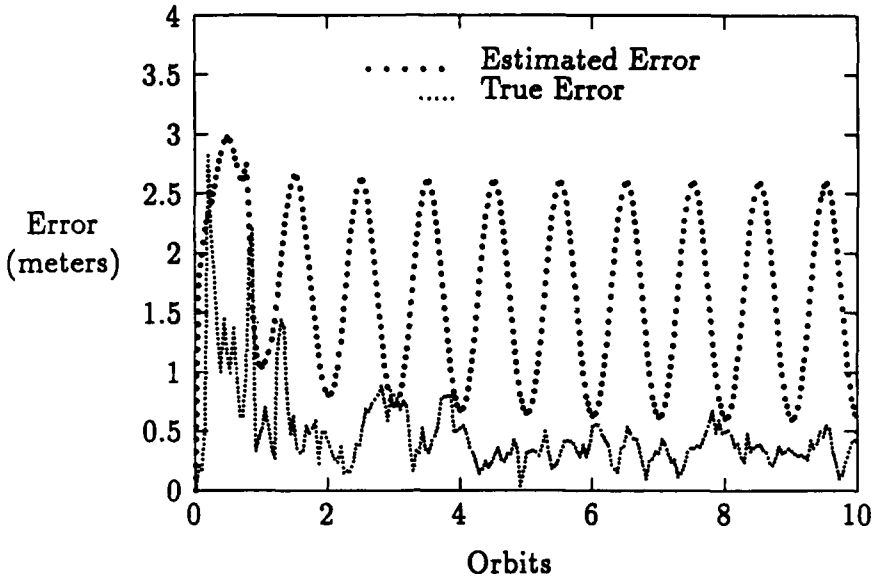

Figure 26. Satellite Ten Error with z and $\dot{z}$ Components Removed

To insure the error propagating backwards remained comparable to the forward error, the state vectors were propagated backwards in same number of steps as it had been propagated forward in time through the use of a counter. The results of this test proved interesting. The conditions used for the run were a two-satellite cluster with the Q_d matrix entries set equal to 1×10^{-10} km for position and 1×10^{-15} $\frac{km}{sec}$ for velocity, five minute update cycles and no noise added to the measurement data. The resulting graphs, Figures 27 - 36, are the exact opposites of each other.

The results of these graphs again indicate the filter cannot observe some or all of the components of the state vector, but it can see linear combinations. The linear combination of a two satellite cluster seems to be the sum of the components rather than their difference. This is the opposite of what was expected.

An observability test was performed to determine if one or more of the eigenvalues were small enough that the associated states can be considered unobservable. The observability test was to calculate the observability Gramian matrix, which has a discrete time representation represented by the following equation (3:243):

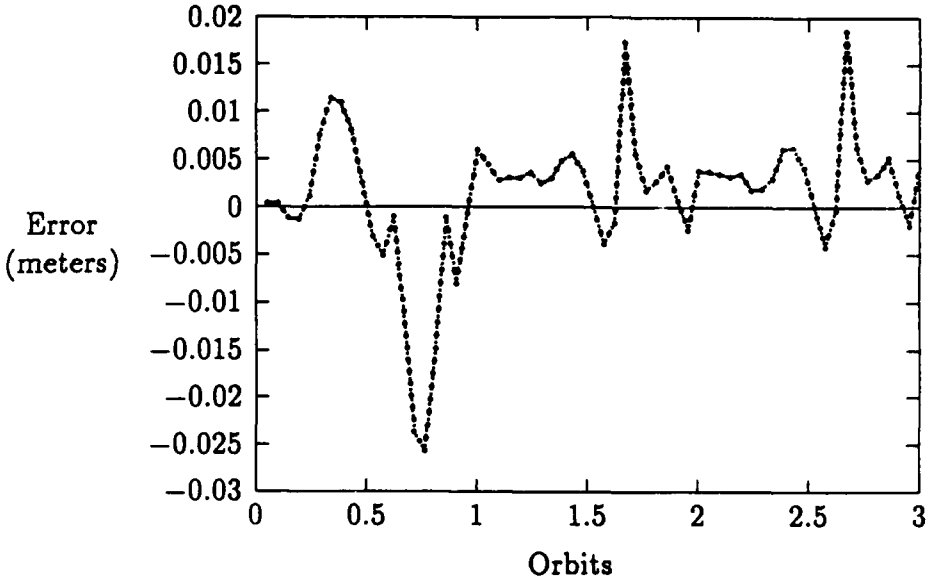

Figure 27. Satellite One Estimated Minus True x Component Values

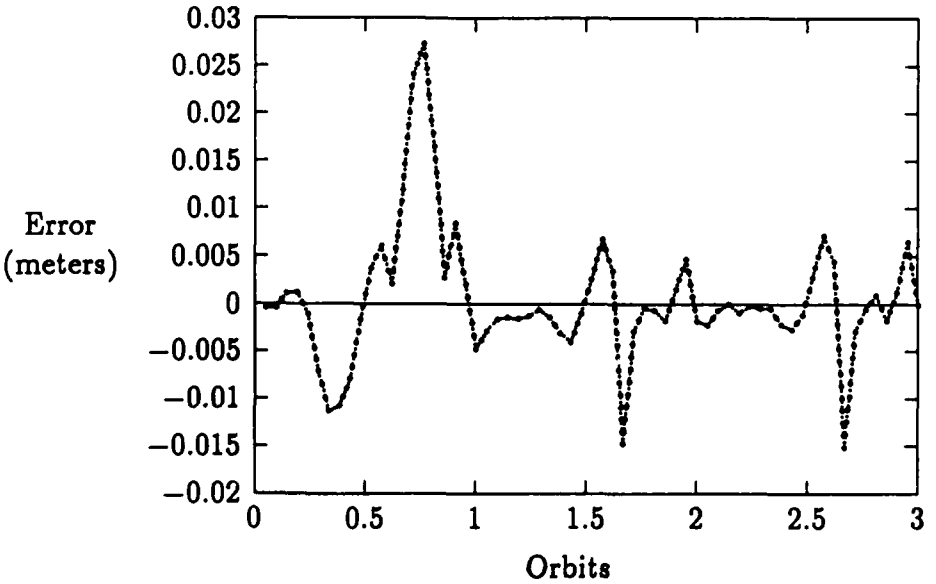

Figure 28. Satellite Two Estimated Minus True x Component Values

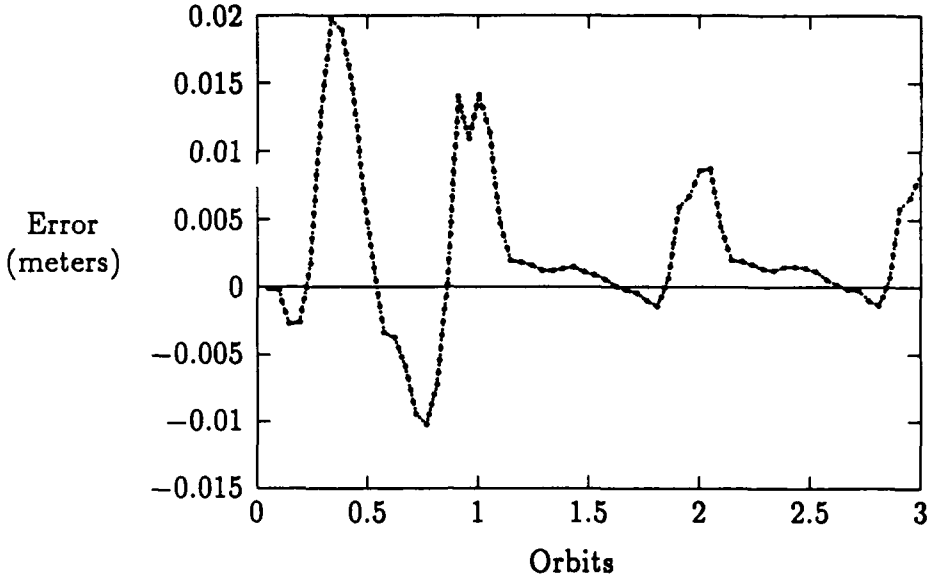

Figure 29. Satellite One Estimated Minus True z Component Values

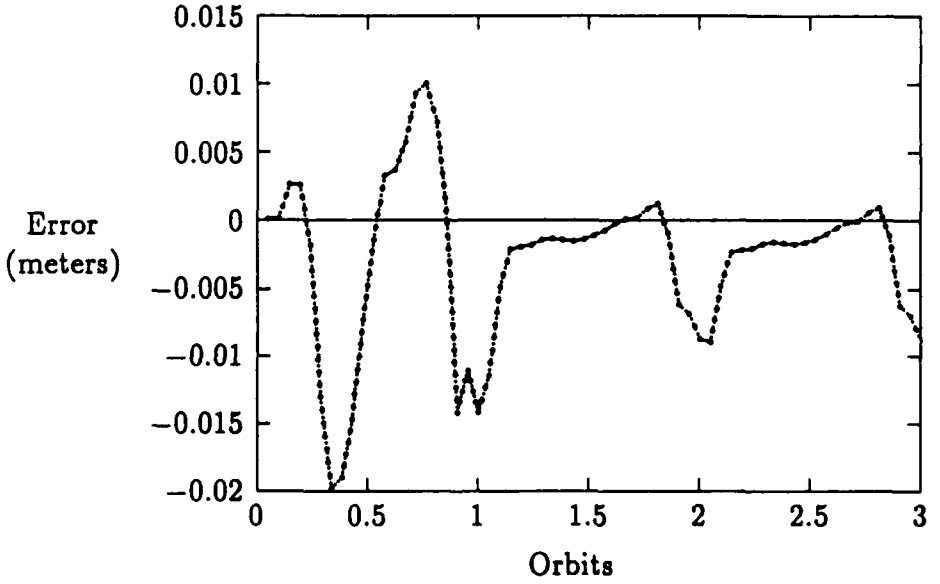

Figure 30. Satellite Two Estimated Minus True z Component Values

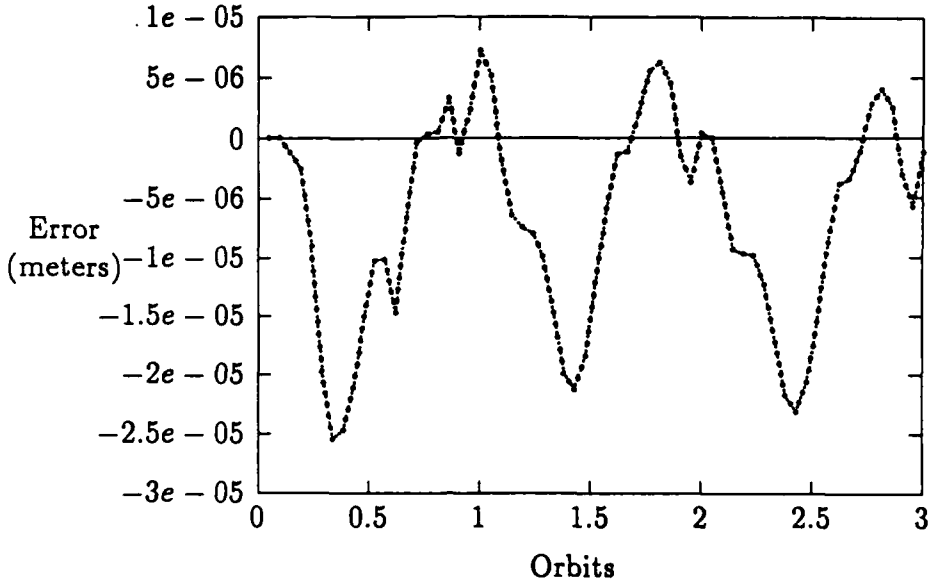

Figure 31. Satellite One Estimated Minus True $\dot{x}$ Component Values

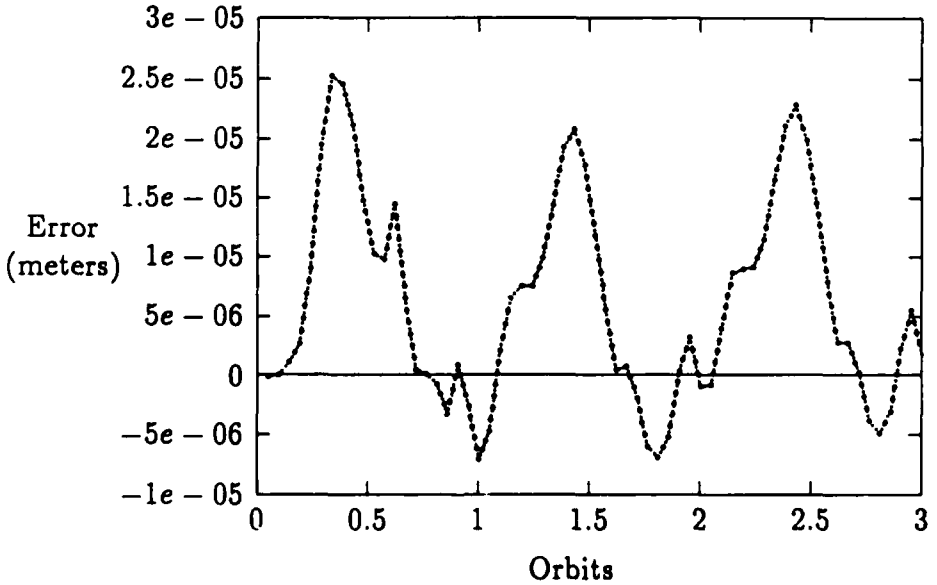

Figure 32. Satellite Two Estimated Minus True $\dot{x}$ Component Values

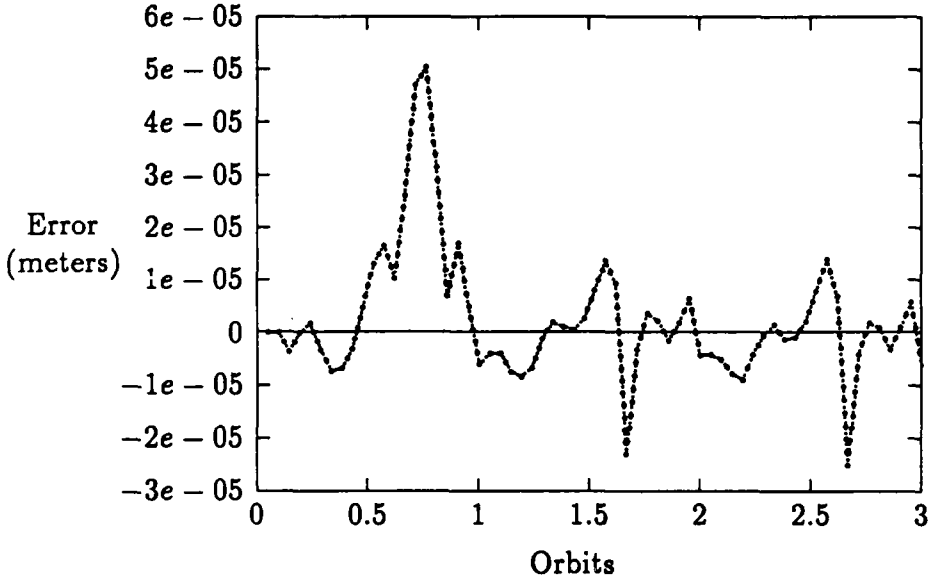

Figure 33. Satellite One Estimated Minus True $\dot{y}$ Component Values

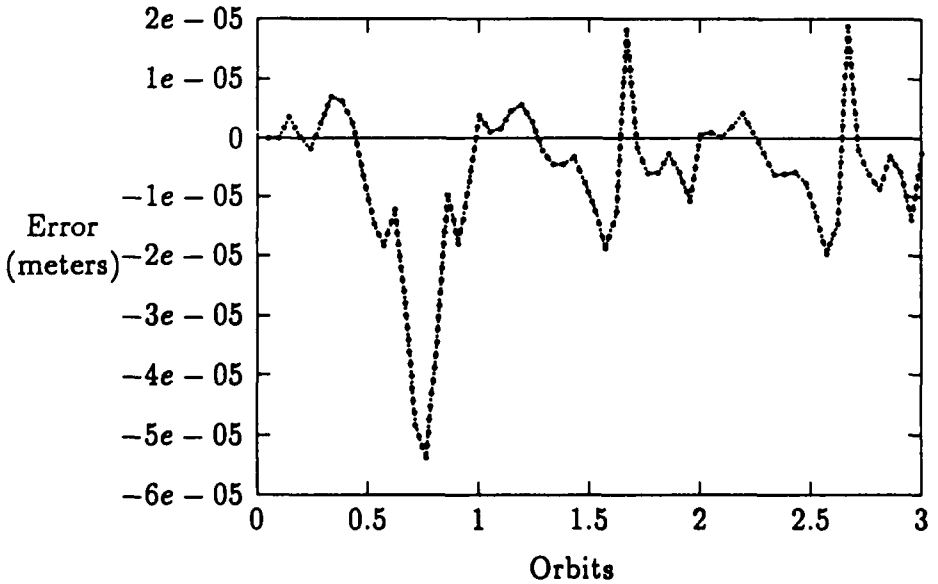

Figure 34. Satellite Two Estimated Minus True $\dot{y}$ Component Values

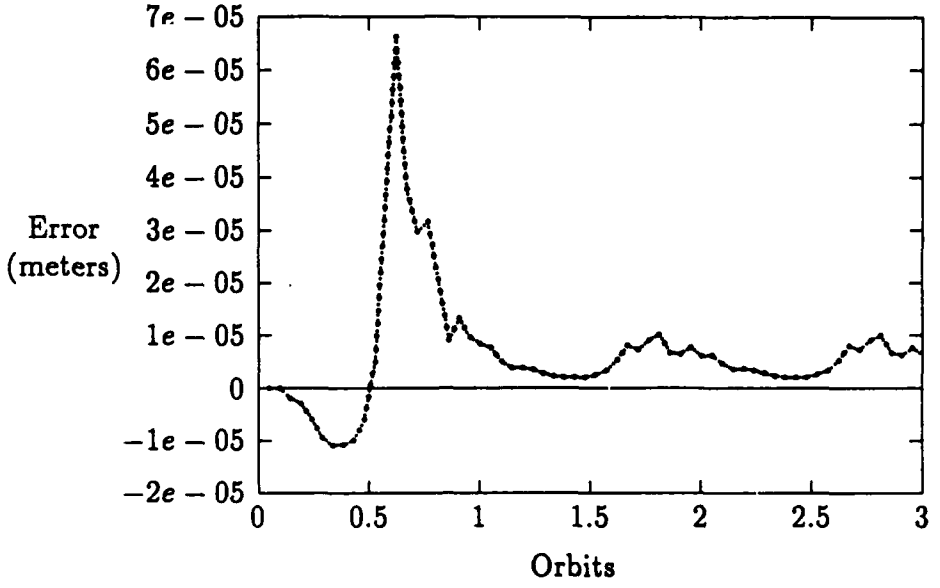

Figure 35. Satellite One Estimated Minus True $\dot{z}$ Component Values

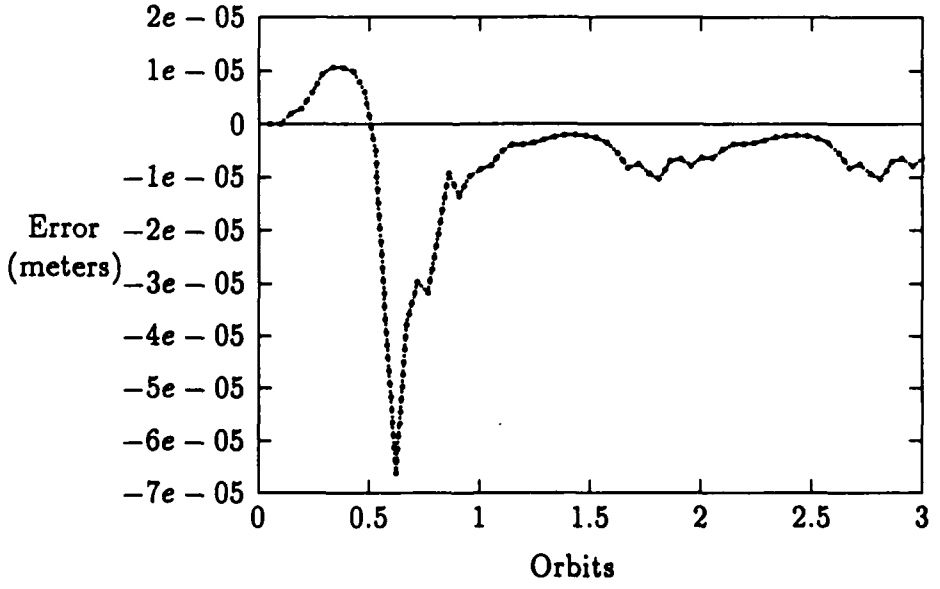

Figure 36. Satellite Two Estimated Minus True $\dot{z}$ Component Values

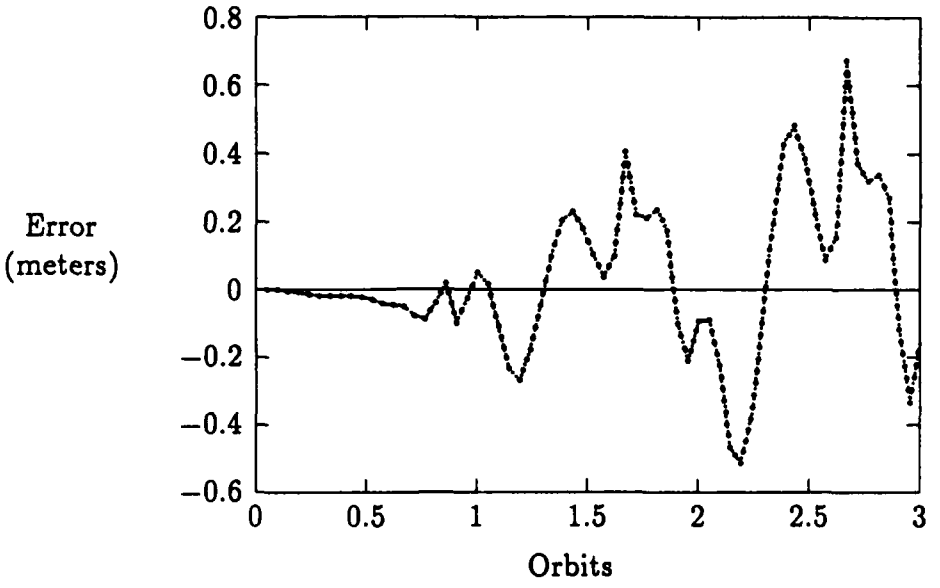

Figure 37. Satellite Two Estimated Minus True Δy Component Values

$$M_D(0,N) \triangleq \sum_{i=1}^{N} \mathbf{\Phi^T}(i,0)\mathbf{H^T}(i)\mathbf{R_f^{-1}}\mathbf{H}(i)\mathbf{\Phi}(i,0) \tag{81}$$

The eigenvalues of the Gramian at different points along the orbit were computed to determine if there was a group of small values that would indicate unobservability. The results of this test showed that no eigenvalue was absolutely zero which would imply that the covariance of that component in the state vector was definitely approaching infinity, but the spread of the eigenvalue exponents made all but three of the values untrustworthy. See Appendix B for the exact values. The test was rerun with the measurements and $\mathbf{\Phi}$ matrix in double precision to attempt to get more accurate results. Even in double precision where the confidence in the values obtained reaches eight decimal places, the eigenvalues obtained still exceeded this spread and again the results imply that only three states can be accurately determined. The numerical stability of the matrix was determined by computing its condition number(3:300). The condition number of a matrix is defined as:

$$k(\mathbf{A}) = \frac{\sigma_{\mathbf{max}}}{\sigma_{\mathbf{min}}} \tag{82}$$

where σ^2_{max} and σ^2_{min} are the maximum and minimum eigenvalues of $\mathbf{A}^{\mathbf{T}}\mathbf{A}$. When the condition number for the observation Gramian matrix was computed, the maximum and minimum eigenvalues were on the order of 10^{25} and 10^{-8}, which results in a condition number of 10^{16}. Studies show numerical difficulties will be experienced as the condition number approaches 10^N where N is the number of significant figures, which for this study was 16. The final conclusion resulting from the observability test is that the filter is ill-conditioned and eight of the states are essentially unobservable since they cannot be determined by the filter and are grouped together as very small numbers.

V. Conclusion

The U-D factorization filter under initial testing met the required accuracy in all the test cases. This initial testing however, did reveal the performance of the filter was different for the satellite with the functioning filter, which was satellite 1 for this study. Under additional testing, this discrepancy was discovered to be caused by the inability of the filter to correctly update the components of the state vector for satellite 1. Additional measurements were sent to the filter residing on satellite 1 but these measurements failed to provide satellite 1 with the necessary information required to update its position components. Observability checks revealed none of the states were definitely unobservable, but eight of the position components were small enough that they could be considered essentially unobservable. Even though the filter has the most difficult time determining the position of satellite 1, the inability of the estimated error to approach the value of the true error for all of the satellites reveals the filter cannot accurately determine the position of any of the satellites in the cluster. Currently, the relative measurement data provided to the filter through the use of the onboard clocks does not supply the filter with the necessary information to determine the relative position from a moving reference point represented by Figure 38.

The true error of the filter is within the required accuracy due to initial values given to the standard deviation of the covariance. This is an artificial means of keeping the true error low. The filter is updating the components it can observe and leaving the remaining states near their steady state values. These steady state values are accurate enough for testing against a truth model based on the two-body equations of motion, but if the filter was placed in an actual space environment with many more disturbance, the inability of the filter to update several of the states would cause the filter to diverge from the true position of the satellites beyond the allowable accuracy.

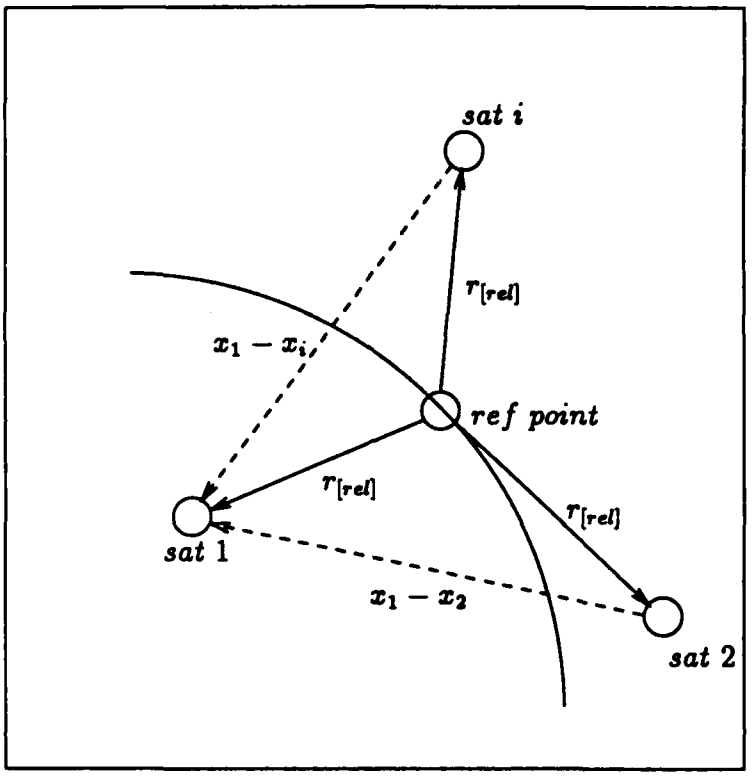

Figure 38. Satellite Cluster Measurement Data and Required Position Determination

With the results obtained from this study, it is obvious the filter is not functioning properly. Since observability checks indicate a large number of the states are essentially unobservable, the development and arrangement system needs to be re-examined from the beginning. Two recommendations for improving the filter include changing the units on the position and velocity components so that their exponential values are closer together and redefining the z component of satellite 1. The first recommendation will reduce the spread of the steady state covariance values which in turn may provide for a more numerically stable system. The second recommendation is to force the z component of satellite 1 to be in the reference orbit

which will force that component to become observable. If these adjustments do not improve the results it may also become necessary to redefine the system to include only relative state components rather than absolute components.

Appendix A. *Satellite True Error Accuracy Requirements*

A.1 Introduction

This appendix outlines the procedure used to determine the accuracy requirements for the Kalman filter. These requirements are used to determine if the estimated position of the satellite is within the required accuracy for a receiver on the ground to obtain a cohesive radar image.

A.2 Accuracy Requirements

As stated in the introduction to this thesis, the accuracy of the filter has been decreased from one quarter of a radar wavelength to one tenth of a radar wavelength to insure the image is clear. The maximum wavelength is a function of the size of the antenna.

According to the problem description, the cluster consists of ten satellites at an altitude of 1000 km. Assuming each satellite has a ground coverage radius of approximately 480 km, the angle subtended at the satellite by the ground is defined as (8:A-1)

$$\tan(\frac{\theta}{2}) = (\frac{480}{1000}) \tag{83}$$

This arrangement is shown in Figure 39. Defining the angle θ as the 3-dB beamwidth and solving for this angle yields

$$\theta_{3dB} = 2\tan^{-1}(\frac{480}{1000}) = .895 \; radians \; or \; 51.282^{\circ} \tag{84}$$

The gain of the system using the value for the 3-dB beamwidth in degrees is (6:86):

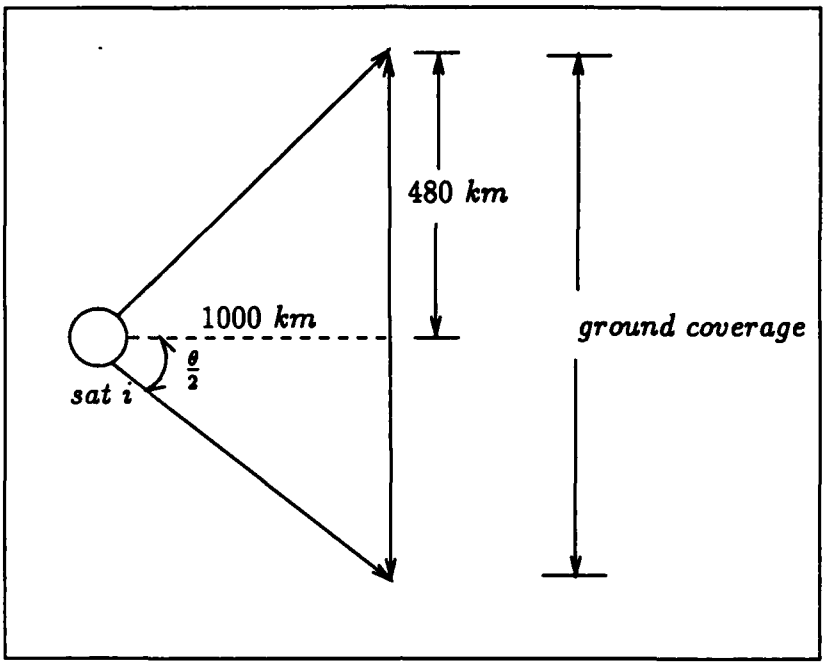

Figure 39. Angle Subtended at the Satellite by the Ground

$$G = \eta(\frac{75\pi}{\theta_{3dB}}) = 11.61 \tag{85}$$

where η is defined as the antenna efficiency and has an assumed value of 55 percent.

If the conservative estimate is made that the overall gain of the cluster is just the multiple of the individual gains then (8:A-1):

$$G_{TOT} = 10 \times G = 116.10 \tag{86}$$

The radar wavelength can then be found by

$$G_{TOT} = \eta(\frac{4\pi A}{\lambda^2}) \tag{87}$$

where A is the area of the satellite cluster defined as $\pi(radius\ of\ the\ cluster)^2$. Rearranging the equation and solving for λ yields

$$\lambda = 2\pi r(\frac{\eta}{G_{TOT}}) \tag{88}$$

For the study presented in this thesis, the radius of the cluster was $.5km$, which when used in the preceding equation yields the following values of the required accuracy of the system:

$$\lambda = 216.23m \tag{89}$$

$$\frac{\lambda}{10} = 21.6m \tag{90}$$

Appendix B. *Observation Matrix Eigenvalue Analysis*

B.1 Introduction

This appendix provides the actual values obtained during the eigenvalue analysis of the observability Gramian. The initial conditions for the test case were five minute updates, steady-state covariance, no noisy data, perfect initial conditions, and driving noise entries equal to $1 \times 10^{-10} km$ for position and $1 \times 10^{-15} \frac{km}{sec}$ for velocity. The filter was allowed to run for three orbits before the analysis was performed to insure that the results were not seriously impacted by the initial transients in the system.

B.2 Eigenvalue Analysis

The eigenvalue analysis was determined first for the U-D factored form of the filter used throughout this thesis. A second filter used to validate the results and check the programming of the first filter was coded using the standard Kalman filter propagation covariance Equation (91) and the extended covariance update Equation (92) with the entire filter in double precision. If the factorization is correct the two results should closely match and validate the conclusion obtained in this thesis.

$$P(-) = \Phi P(+) \Phi + G_d Q_d G_d^T \tag{91}$$

$$P(+) = P(-) - KHP(-) \tag{92}$$

where K is defined as

$$K = P(-) H^T \left[HP(-) H^T + R_f \right]^{-1} \tag{93}$$

The covariance values from each of the filters were checked against each other in a two-satellite cluster and they matched. With the results of the new filter verified the observability Gramian was computed. The resulting eigenvalues for the observability Gramian in a two satellite cluster running for three orbital periods were as follows:

$$U-D\ filter \begin{bmatrix} -.246\times10^{-9} \\ -.183\times10^{-10} \\ -.373\times10^{-14} \\ -.140\times10^{-15} \\ .209\times10^{-16} \\ .842\times10^{-14} \\ .710\times10^{-12} \\ .591\times10^{-10} \\ .903\times10^{4} \\ .414\times10^{7} \\ .717\times10^{7} \end{bmatrix} \quad and\ Standard\ Filter \begin{bmatrix} -.265\times10^{-12} \\ -.522\times10^{-14} \\ -.295\times10^{-14} \\ -.148\times10^{-20} \\ -.148\times10^{-20} \\ .228\times10^{-15} \\ .689\times10^{-11} \\ .743\times10^{-11} \\ .903\times10^{4} \\ .414\times10^{7} \\ .717\times10^{7} \end{bmatrix} \tag{94}$$

The test run for the first filter indicates that the first eight eigenvalues are outside the eight decimal place limit from the maximum exponential value that can be trusted with double precision accuracy. The last three values are the only values that are within this limit. These results were validated with the second filter. The agreement and accuracy of the last three eigenvalues indicates that these are the only states that the filter can accurately represent. Since the first eight eigenvalues are very small they can be considered essentially zero and represent the (essentially) unobservable states.

Bibliography

1. Bate, Roger and others. *Fundamentals of Astrodynamics*. New York: Dover Publications, 1971.
2. Jacobs, Donald H. *Fundamentals of Optical Engineering*. New York: McGraw-Hill Book Company, 1943.
3. Maybeck, Peter S. *Stochastic Models, Estimation, and Control Volume 1*. New York: Academic Press, 1979.
4. Maybeck, Peter S. *Stochastic Models, Estimation, and Control Volume 2*. New York: Academic Press, 1982.
5. Murdoch, John. "Cooperative Orbit Control Strategies For Colocated Geostationary Satellite." In *AAS-85-375, AIAA/AAS Astrodynamcis Conference*, pages 831–852, Vail Colorado: AIAA, 1985.
6. Roddy, Dennis. *Satellite Communications*. Englewood Cliffs, New Jersey: Prentice Hall, 1989.
7. Swinerd, Graham and John Murdoch. "An Assessment of Satellite-To-Satellite Tracking Applied To Satellite Cluster." In *Proceeding of the Astrodynamics 1985 Conference*, pages 1001–1018, San Diego: Univelt, Inc., 1986.
8. Ward, Captain Michael L. P. *Estimated Satellite Cluster Elements in Near Circular Orbit*. MS thesis, AFIT/GA/AA/88D-13, School of Engineering, Air Force Institute of Technology (AU), Wright-Patterson AFB OH, December 1988.
9. Wiesel, William B. Class Handout distributed in MECH 731, Modern Methods of Orbit Determination. School of Engineering, Air Force Institute of Technology (AU), Wright-Patterson AFB OH, April 1989.
10. Wiesel, William B. *Spaceflight Dynamics*. New York: McGraw-Hill, 1989.

Vita

Captain Sherrie Filer [redacted]. She graduated from Pueblo High School in Pueblo, Colorado in 1980. Later she attended the United States Air Force Academy, from which she received a degree of Bachelor of Science in Engineering Sciences. Upon graduation, she received a USAF commission and traveled to Wright Patterson AFB to work in the Flight Dynamics Laboratory. She served as a flight test engineer for a coupled weapon delivery system on an F-15 aircraft. In May 1988, she entered the School of Engineering at the Air Force Institute of Technology.

[redacted]

REPORT DOCUMENTATION PAGE

Form Approved
OMB No. 0704-0188

1a. REPORT SECURITY CLASSIFICATION: UNCLASSIFIED	1b. RESTRICTIVE MARKINGS
2a. SECURITY CLASSIFICATION AUTHORITY	3. DISTRIBUTION / AVAILABILITY OF REPORT: Approved for public release; distribution unlimited
2b. DECLASSIFICATION / DOWNGRADING SCHEDULE	
4. PERFORMING ORGANIZATION REPORT NUMBER(S): AFIT/GA/ENY/89D-2	5. MONITORING ORGANIZATION REPORT NUMBER(S)
6a. NAME OF PERFORMING ORGANIZATION: School of Engineering; 6b. OFFICE SYMBOL (If applicable): AFIT/ENY	7a. NAME OF MONITORING ORGANIZATION
6c. ADDRESS (City, State, and ZIP Code): Air Force Institute of Technology, Wright-Patterson AFB, OH 45433-6583	7b. ADDRESS (City, State, and ZIP Code)
8a. NAME OF FUNDING / SPONSORING ORGANIZATION; 8b. OFFICE SYMBOL (If applicable)	9. PROCUREMENT INSTRUMENT IDENTIFICATION NUMBER
8c. ADDRESS (City, State, and ZIP Code)	10. SOURCE OF FUNDING NUMBERS: PROGRAM ELEMENT NO. / PROJECT NO. / TASK NO / WORK UNIT ACCESSION NO.

11. TITLE (Include Security Classification)
INVESTIGATION OF THE OBSERVABILITY OF A SATELLITE CLUSTER IN A NEAR CIRCULAR ORBIT

12. PERSONAL AUTHOR(S)
Sherrie N. Filer, B.S., Capt, USAF

13a. TYPE OF REPORT	13b. TIME COVERED	14. DATE OF REPORT (Year, Month, Day)	15. PAGE COUNT
MS Thesis	FROM _____ TO _____	1989, December	61

16. SUPPLEMENTARY NOTATION

17. COSATI CODES			18. SUBJECT TERMS (Continue on reverse if necessary and identify by block number)
FIELD	GROUP	SUB-GROUP	Satellite Cluster Kalman Filter
22	03		

19. ABSTRACT (Continue on reverse if necessary and identify by block number)

Thesis Advisor: William E. Wiesel
Professor
Department of Aeronautics and Astronautics

20. DISTRIBUTION / AVAILABILITY OF ABSTRACT: ☒ UNCLASSIFIED/UNLIMITED ☐ SAME AS RPT ☐ DTIC USERS	21. ABSTRACT SECURITY CLASSIFICATION: UNCLASSIFIED
22a. NAME OF RESPONSIBLE INDIVIDUAL: William E. Wiesel, Professor	22b. TELEPHONE (Include Area Code): (513) 255-3069 / 22c. OFFICE SYMBOL: AFIT/ENY

DD Form 1473, JUN 86 — Previous editions are obsolete.

The relative position determination of a cluster of satellites in a near circular orbit was investigated in a thesis by Captain Michael L. P. Ward in December 1988. His investigation involved the use of dynamics based on the Clohessy-Wiltshire equations and an on-board estimator based on the U-D covariance factorization version of the Kalman filter. The initial performance results proved favorable, with the filter meeting the required 25 meter accuracy in all test cases. The purpose of this thesis is to validate the test results achieved by Captain Ward and to investigate the ability of the filter to determine the relative position of the satellites to a higher degree when the filter in use is not resident on that satellite. This investigation included the use of additional measurement data from other satellites in the cluster to the Kalman filter for processing in the update cycle. When it was determined that the measurements were not allowing satellite 1 to update, the observability of the components of the state vector were computed and the results discussed.